CONFIDENTIAL
RESTRICTED DATA
Atomic Energy Act

MASTER

WANL-TME-1151

Westinghouse Astronuclear Laboratory

HYDROGEN CORROSION OF GRAPHITE MATERIALS AND GRAPHITE REACTOR COMPONENTS

(Title Unclassified)

DISTRIBUTION OF THIS DOCUMENT IS UNLIMITED

CONFIDENTIAL
RESTRICTED DATA
Atomic Energy Act

21

~~CONFIDENTIAL~~
~~RESTRICTED DATA~~
~~Atomic Energy Act - 1954~~

~~GROUP 1~~

~~Excluded From Automatic Downgrading and Declassification~~

76

Astronuclear Laboratory

WANL-TME-1151

NOTICE

This report was prepared as an account of work sponsored by the United States Government. Neither the United States nor the United States Energy Research and Development Administration, nor any of their employees, nor any of their contractors, subcontractors, or their employees, makes any warranty, express or implied, or assumes any legal liability or responsibility for the accuracy, completeness or usefulness of any information, apparatus, product or process disclosed, or represents that its use would not infringe privately owned rights.

MASTER

HYDROGEN CORROSION OF GRAPHITE MATERIALS AND GRAPHITE REACTOR COMPONENTS

(Title Unclassified)

by

J. W. H. Chi
Fluid Flow Laboratory
Experimental Engineering Department

Classification cancelled for changed to
by authority of DOC
by HAC, T.C. date SEP 10 1973

Approved By:

E. A. DeZuboy, Manager
Fluid Flow Laboratory

~~INFORMATION CATEGORY~~

~~CONFIDENTIAL - N.D.~~

6/9/65

Authorized Classifier Date

~~CONFIDENTIAL~~
~~RESTRICTED DATA~~
~~Atomic Energy Act - 1954~~

CONFIDENTIAL
RESTRICTED DATA
Atomic Energy Act - 1954

SUMMARY

Experimental data reported in the literature on hydrogen reactions with (or corrosion of) graphite materials have been analyzed in an attempt to 1) better understand the mechanisms of the reactions involved, and 2) develop rate equations and reaction velocity constants for engineering analysis.

The thermodynamics of the system carbon-hydrogen was first studied and lead to the conclusion that in the range of temperatures and pressures of concern in the NERVA reactor, both methane and acetylene reactions must be taken into account. At temperatures below approximately 3800°R, the primary reaction is methane formation. However, at temperatures greater than approximately 3800°R, acetylene formation predominates.

It was postulated that the rate equations for the met e and acetylene reactions are first order with respect to hydrogen. On this basis, reaction velocity constants were calculated from corrosion data obtained for the following materials and experimental conditions:

Materials:	AUC, H4LM, SPK, ATJ, UO_2 - Fueled and unfueled, and other unspecified graphites.
Temperature:	1800 to 6459°R
Pressure:	.0016 to 1100 psia
Mass Flowrate:	.07 to .80 lb/in^2-sec

The results, presented on an Arhenius plot, showed excellent correlations. The following important facts were observed:

1) The activation energies for both fueled and unfueled graphites are the same.

2) There is no significant difference in reaction velocity constants for the unfueled graphite materials.

CONFIDENTIAL
RESTRICTED DATA
Atomic Energy Act - 1954

3) The apparent reaction velocity constants for fueled graphites are higher than those for the unfueled; the constants increasing with increased fuel loadings.

4) The activation energy for the acetylene reaction is higher than that for the methane reactions.

5) The corrosion rate of pyrographite is unique. Below 4000°R, the reaction velocity constants were significantly lower than those for normal graphite. But, above 4000°R, they were the same.

The higher corrosion rates observed for fueled graphite was attributed to erosion effects resulting from the physical removal of non-reacting fuel beads which contributes to the overall weight loss or surface regression of the material. An empirical equation was proposed to account for erosion as a function of the fuel loading and mass velocity.

The higher activation energy observed for the acetylene reaction suggests that if reactors were to be operated at temperatures higher than those presently designed, acetylene formation will be potentially the more serious of the two corrosion reactions.

As independent checks on the validity of the rate equations and the reaction velocity correlations developed, hydrogen corrosion of graphite reactor components were analyzed. The experimental data available are the following:

1) Isothermal corrosion of unfueled, uncoated, 19-hole elements.

2) Center hex corrosion from a single-cluster corrosion test carried out in the A-10 furnace.

3) Fifty-six (56) inch long AUC graphite annulus (.010-inch gap).

4) Uncoated coolant channels in a UC_2-fueled, 19-hole element, tested in the A-2 furnace.

The results showed excellent agreements in general between calculated and observed local corrosion data and between calculated and observed overall weight losses. The small

deviations observed can be attributed to the fact that erosion effects on unfueled graphites were neglected.

Possible mechanisms of the corrosion reactions were discussed, and rate equations were derived on the basis of a surface reaction mechanism. The theoretical equations were shown to be consistent with the empirically developed phenomenological equations. Rates of diffusion were calculated and compared with the apparent reaction rates. The results showed that the rates of diffusion were significantly greater, thus providing further evidence on the validity of the surface reaction mechanisms.

The recommended reaction velocity constants for the methane and acetylene reactions are:

$$k_1 = 8.975 \exp(-48{,}900/RT) \text{ in/sec} \qquad \text{(methane)}$$

and

$$k_2 = 574 \exp(-88{,}000/RT) \text{ in/sec} \qquad \text{(acetylene)}$$

where

$R = 1.9872$, and T is in $^{\circ}R$.

On the basis of the excellent correlations obtained on data taken from a variety of graphite materials and flow geometries, it is felt that the reaction velocity constants recommended can be used with confidence in the analysis and design of NERVA reactors.

The effects of radiation and heat of reaction on the rate of corrosion were briefly discussed and areas where further experimental studies are required were suggested.

The application of corrosion measurements to high temperature determinations were illustrated, and a simple equation for the calculation of maximum local corrosion rates was given.

CONFIDENTIAL
RESTRICTED DATA
Atomic Energy Act - 1954

TABLE OF CONTENTS

	Page
Summary	ii
List of Tables	vii
List of Figures	viii
Introduction	1
Thermodynamics of the H_2-C System	3
Previous Work and Experimental Data	3
Development of Rate Equations	8
Methane Formation	9
Acetylene Formation	10
Testing the Rate Equations	11
Further Verification of the Correlations	15
Effect of Physical and Chemical Erosion on Overall Corrosion or Graphite	20
Effect of Fuel Loading on Corrosion	20
Corrosion of Pyrographite	23
Hydrogen Corrosion of Graphite Components	24
Unfueled Elements	24
AUC - Graphite Annulus	26
Uncoated Coolant Channels	28
Center Hex Corrosion	28
Discussions	32
Corrosion Measurements as Aid to Analysis	32
Mechanisms of Hydrogenation Reactions	34
Rates of Bulk Diffusion and Pore Diffusion	38
Carbon Deposition	38

CONFIDENTIAL
RESTRICTED DATA
Atomic Energy Act - 1954

TABLE OF CONTENTS (CONTINUED)

	Page
Effect of Radiation	39
Heats of Reaction	39
Maximum Local Rate of Corrosion	40
Recommended Experimental Studies	41
Conclusions	42
Acknowledgments	44
Nomenclature	45
References	47
Appendix I	49
Appendix II	51
Appendix III	55
Appendix IV	57
Appendix V	59
Appendix VI	62

CONFIDENTIAL
RESTRICTED DATA
Atomic Energy Act - 1954

LIST OF TABLES

Table No.	Title	Page
I	LASL Corrosion Tests on Unloaded, 19-Hole Hexes	64
II	Corrosion of AUC Annulus 1-1/8 Inch Diameter, .010 Inch Gap	65
III	Corrosion of Uncoated Coolant Channels	66
IV	Corrosion of Unlined Support Block (ATJ Graphite, Sp. Gr. = 1.73) 500 psia	67

CONFIDENTIAL
RESTRICTED DATA
Atomic Energy Act - 1954

BLANK PAGE

LIST OF FIGURES

Figure No.	Title	Page
1	Equilibrium Constants for the Most Probable Hydrogenation Reactions	4
2	Relative Equilibrium Concentrations of Methane and Acetylene	5
3	Comparisons of Experimental Conditions for Various Sources of Data	6
4	Arhenius Correlation on Apparent Reaction Velocity Constants for First Order Rate Equations	14
5	Effect of Fuel Loading on Reaction Velocity Constants	16
6	Comparison of Reaction Velocity Constants Calculated From High and Low Pressure Data	19
7	Comparisons of Observed and Calculated Overall Weight Loss - 19-Hole Uncoated and Unfueled Elements	25
8	Comparison of Calculated and Experimental Local Corrosion Rates AUC Graphite Annulus - .010 Inch Gap	27
9	Comparison of Observed and Calculated Local Corrosion Rates Uncoated, NRX-A2 Type Fueled Coolant Channels - A-2 Furnace Run 331	29
10	Observed and Calculated Temperatures in the Single Cluster Corrosion Test	31
11	Comparison of Observed and Calculated Center Hex Corrosion (Graphite Annulus)	33

CONFIDENTIAL
RESTRICTED DATA
Atomic Energy Act - 1954

INTRODUCTION

Recent KIWI B-4D, B-4E and NRX-A2 tests have clearly shown that hydrogen corrosion of unprotected graphite is a serious problem in those reactors. Since succeeding NERVA reactors and other advanced reactors are expected to be tested or operated for longer periods and higher temperatures than those of the past, the prevention of corrosion in NERVA reactors is of critical concern. It was recognized that systematic analysis and prediction of hydrogen corrosion of reactor components are required in order to improve reactor design and to correctly interpret component and reactor test data. Such analyses, however, require as a prerequisite a knowledge of the kinetics of the chemical reactions involved. Although a large number of experimental studies have been carried out on various hydrogen-graphite systems, the results have shown large discrepancies and an apparent lack of correlation among all the data. This has been generally attributed to the complexity of the systems involved, differences in physical and chemical properties among the different materials, etc. In addition, the data presented cannot be used directly for engineering analysis. Consequently, all the available data on hydrogen-graphite systems are analyzed in this report in an atrempt to

1) better understand the mechanisms of corrosion,

2) develop general rate equations,

3) develop general correlations for reaction velocity constants, and

4) demonstrate their validity and their use by the analysis and calculation of hydrogen corrosion of graphite reactor components and comparing them with experimental results.

In a flow system (such as those of concern in the NERVA reactor), a simple material balance on carbon in the bulk gaseous stream yields at steady-state, the equation

$$\sum r_i \, dZ = d(y_c N) \qquad (1)$$

CONFIDENTIAL
RESTRICTED DATA
Atomic Energy Act - 1954

where $\sum r_i$ is the sum of the local rates of hydrocarbon formations, y_c is the mole fraction carbon in the gas, and N is the total gaseous molar flowrate at any location Z.

The local rate of corrosion can be determined from a carbon balance on the graphite wall

$$\frac{dr}{dt} = a \left(\sum a_i r_i + b r_e \right) \tag{2}$$

where r is the corrosion in units of length, a, a_i, and b are constants, and r_e is the rate of erosion. But the local rates of hydrocarbon formation are, in general, functions of the local temperature, pressure, and reactant and product concentrations, while the determination of the local reactant and product concentrations requires a knowledge of the local flowrate and upstream conditions. The rate of erosion, r_e, is expected to be a function of the fluid velocity, surface condition, etc. Consequently, an analysis of hydrogen corrosion of graphite in a nuclear reactor and reactor components requires

1) basic rate equations and their relationships to the variables mentioned above,

2) an integration of the flow-reaction Equation (1) with known temperature, pressure, and flow distributions to determine the local reactant and product concentrations, and

3) calculation of the local corrosion rates from Equation (2).

The determination of the basic rate equations requires in turn a knowledge of

1) the chemical reactions taking place, and

2) the mechanism(s) of the reactions.

As a first step towards the development of rate equations, the thermodynamics of the hydrogen-carbon system shall be examined.

CONFIDENTIAL
RESTRICTED DATA
Atomic Energy Act - 1954

THERMODYNAMICS OF THE H_2-C SYSTEM

In the range of temperatures and pressures of concern in the reactor, the primary reaction products are methane, acetylene, ethylene, and ethane. As a comparison of the relative stability of these hydrocarbons, the logarithm of the equilibrium constants (in terms of partial pressures) are plotted versus the reciprocal of the absolute temperature as shown in Figure 1. It is evident from this figure that methane and ethane become increasingly unstable at higher temperatures, whereas the opposite is true of acetylene and ethylene. However, since the equilibrium constants of methane are significantly higher than those of the other hydrocarbons at low temperatures, while those of acetylene are significantly higher than those of all other products at high temperatures, the formation of only these two are of primary concern in the reactor. For a further comparison on the relative importance of methane and acetylene, the ratio of the equilibrium mole fractions of methane to acetylene are plotted versus the temperature at constant pressures as shown in Figure 2.

It is evident from this plot that at low pressures, acetylene becomes important at relatively low temperatures, while at higher pressures, the appearance of acetylene does not become significant until higher temperatures are attained.

PREVIOUS WORK AND EXPERIMENTAL DATA

Figure 3 presents the sources of experimental data on various types of graphite and the ranges of experimental conditions studied. Note that among the data available, only those of Hedden,[1] Landahl,[5] and Landahl[6] were carried out over appreciable ranges of pressure (130-1100 psia). From thermodynamic considerations, it can be shown that the data in Reference 1 were carried out under conditions that produced primarily the methane reaction whereas for the conditions studied by Gulbranson[2] acetylene production is expected to be dominant. Finally, the wide pressure range covered by the data in Reference 6 suggests that both methane and acetylene reactions can be expected. Since the order of the rates of reactions is determined from the pressure dependency and the exponent of the

CONFIDENTIAL
RESTRICTED DATA
Atomic Energy Act - 1954

CONFIDENTIAL
RESTRICTED DATA
Atomic Energy Act - 1954

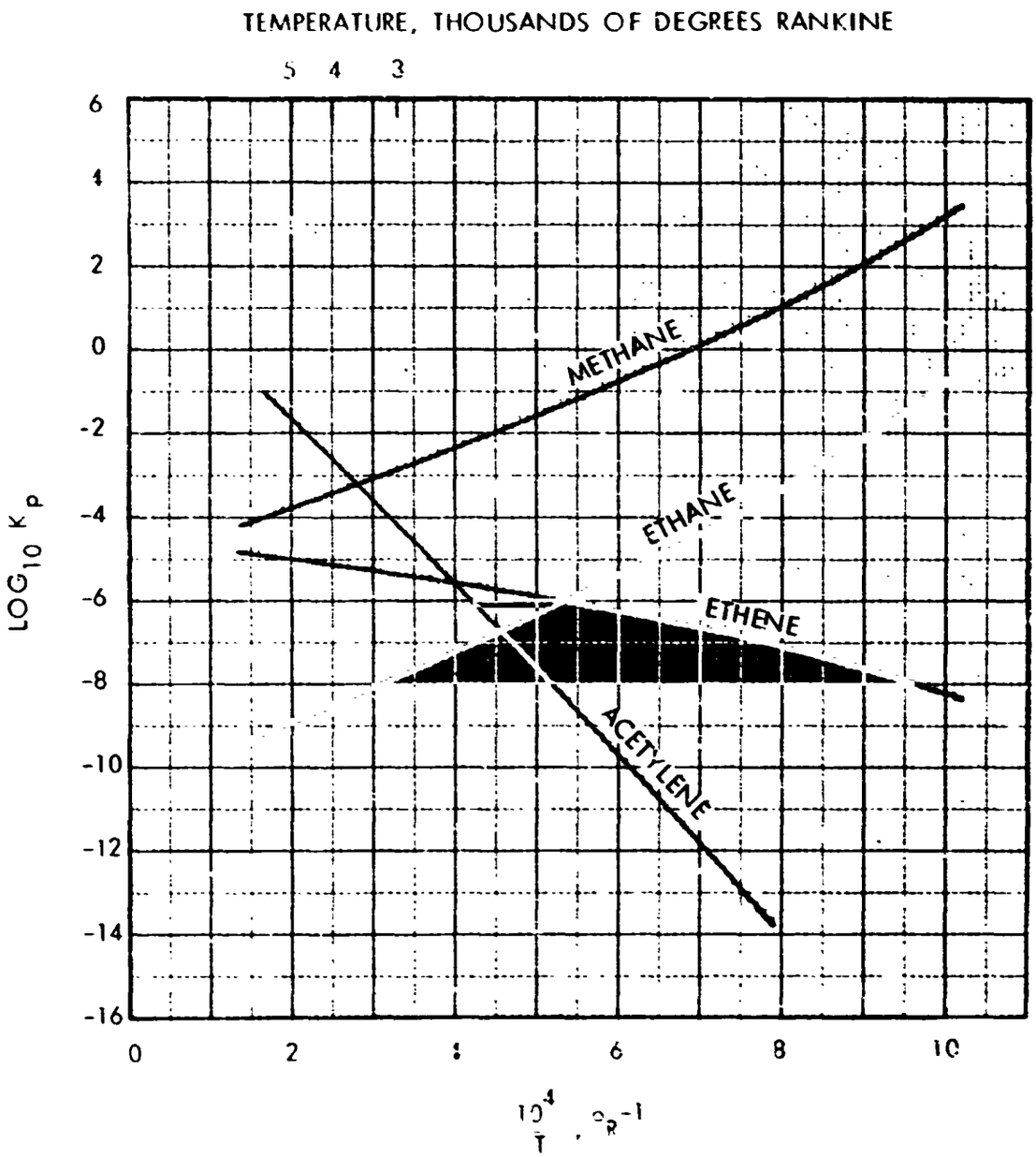

Figure 1

Equilibrium Constants for the Most Probable Hydrogenation Reactions

CONFIDENTIAL
RESTRICTED DATA
Atomic Energy Act - 1954

CONFIDENTIAL
RESTRICTED DATA
Atomic Energy Act - 1954

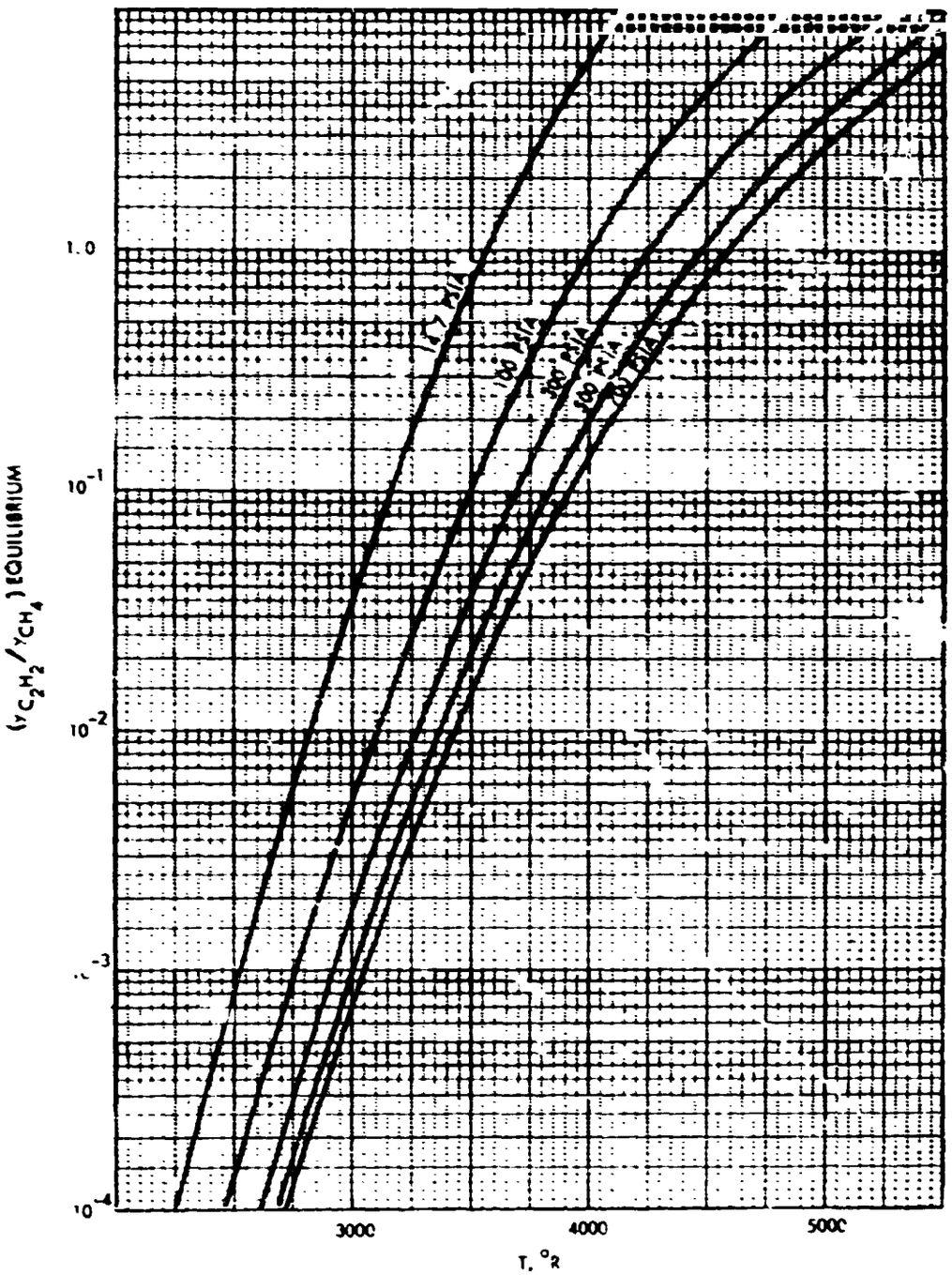

Figure 2

Relative Equilibrium Concentrations of Methane and Acetylene

CONFIDENTIAL
RESTRICTED DATA
Atomic Energy Act - 1954

CONFIDENTIAL
RESTRICTED DATA
Atomic Energy Act - 1954

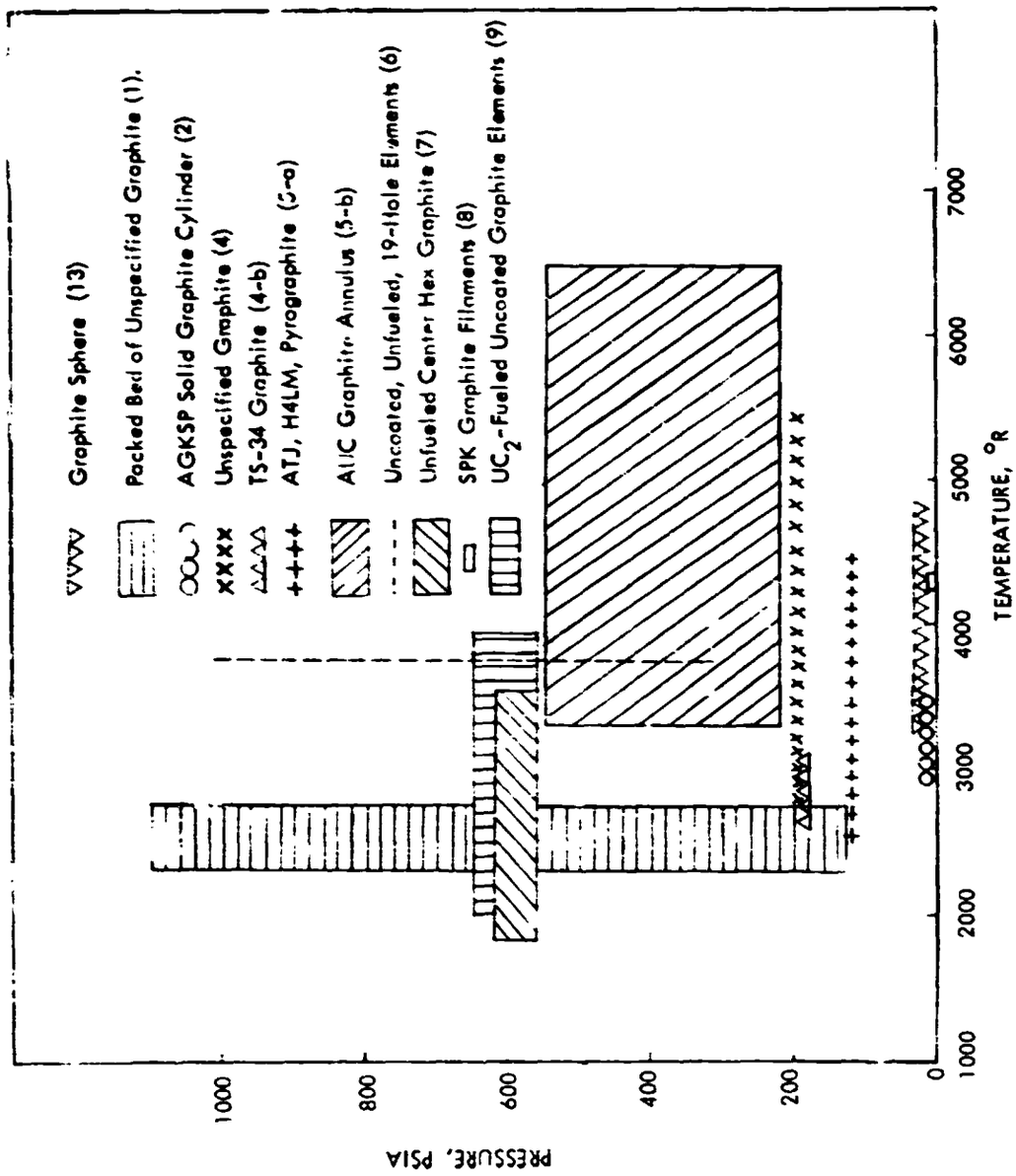

Figure 3

Comparisons of Experimental Conditions for Various Sources of Data

CONFIDENTIAL
RESTRICTED DATA
Atomic Energy Act - 1954

pressure, the data from References 1 and 5 were used primarily for the determination of the "order" of the methane and acetylene reactions. The data from Reference 6 were used as independent checks.

Note that the data from Rogers and Sesonske,[4] Landahl,[5] Lowrie,[8] and Landahl[10] were obtained over a wide range of temperatures (2550 to 6450°R) and with a wide variety of graphitic materials. Consequently, these were used to obtain correlations for the reaction velocity constants.*

Gulbransen et. al.[2] carried out their study in an alumina tube. Complicating side reactions, producing O_2, CO, and CO_2 were found to occur. Since the reaction rates were determined from graphite weight losses, the weight loss due to hydrocarbon formation could not be separated from those due to the side reactions. In view of these facts, the results from this work were not used in the analysis to follow. The data on SPK graphite[8] were taken at extremely low pressures (1.2 to 4.1 Torr). Although the data were very limited, they were reported in such a manner that absolute reaction velocity constants can be calculated.

The remaining sets of data obtained from component tests (uncoated fuel elements, uncoated, fueled coolant channels, and graphite annulus) will be used as independent checks on the rate equations to be developed and on the reaction velocity correlations.

---

* The reaction velocity constant is a function of the temperature only.

DEVELOPMENT OF RATE EQUATIONS

The general mechanisms of heterogeneous gas-solid reactions are well known. These involve the following successive steps:

1) diffusion of hydrogen from the bulk stream to the fluid-solid interface,

2) diffusion of hydrogen through the pores,

3) adsorption of hydrogen on the solid surface,

4) surface reaction,

5) desorption of reaction product(s),

6) diffusion out of the pores, and

7) diffusion of reaction products from the gas-solid interface to the bulk stream.

If any one of the above steps is significantly slower than the others, then it is the rate-controlling step. The general procedure for the determination of a rate equation is to 1) postulate a mechanism or mechanisms, 2) derive the rate equation, and 3) compare with the experimental data. Hence, the development of a rate equation for any particular reaction involves a trial and error procedure.

In their studies on the hydrogen-graphite or hydrogen-carbon systems, Zielke and Gorin,[3] Hedden,[1] and Rogers and Sesonske[4] have postulated chemisorption or surface reaction rate controlling mechanisms. Both Hedden and Rogers and Sesonske have pointed out the complexity of the hydrogen-graphite system and the fact that inumerable rate equations can be derived on the basis of Step 4 alone! But the validity of the rate equation(s) must be corroborated by the experimental data.

In view of these facts and the often hopeless task of determining the actual rate-controlling mechanism(s), it is common practice to determine empirically the "order" of the reaction. By this approach, a phenomenological rate equation can be obtained.

CONFIDENTIAL
RESTRICTED DATA
Atomic Energy Act - 1954

Methane Formation

On this basis, Hedden[1] showed conclusively that the rate of methane formation is first order with respect to hydrogen. However, from data taken over a very limited pressure range, Rogers and Sesonske[4] concluded that the rate of corrosion of graphite is of zero order with respect to hydrogen. Rogers and Sesonske did not measure hydrocarbon concentrations, but based their rate equation entirely on the methane reaction. It can be readily seen from Figure 2 that at the temperatures and pressures investigated by Rogers and Sesonske, acetylene formation cannot be nealected. This may explain the apparent zero order rate equation determined by Rogers and Sesonske for methane formation.

Hedden showed that the first order rate equation is compatible with the rate equation derived by Zielke and Gorin,[3] who studied the hydrogenation of chars. Hedden obtained his kinetic data from a packed bed of graphite particles. It was postulated that the rate of methane formation is proportional to the mass of the graphite present. But, such a rate equation cannot be applied to systems other than that studied. For a more general rate equation, it is postulated here that the rate of methane formation is proportional to the gross external surface area; whence,

$$\frac{d\,n_{CH_4}}{d\,t} = k_1\,S\left(C_{H_2} - \frac{C_{CH_4}}{K_1\,C_{H_2}}\right) \tag{3}$$

where k_1 is the forward reaction velocity constant in the methane reaction

$$C + 2\,H_2 \underset{k_1'}{\overset{k_1}{\rightleftharpoons}} CH_4 \tag{4}$$

CONFIDENTIAL
RESTRICTED DATA
Atomic Energy Act - 1954

and K_1 is the equilibrium constant in terms of concentrations:

$$K_1 = \frac{k_1}{k_1'} = \left(\frac{C_{CH_4}}{C_{H_2}^{\,2}}\right)_{equil.} \tag{5}$$

Acetylene Formation

Although at the temperatures and pressures studied by Rogers and Sesonske[4] and Gulbransen et al,[2] acetylene is expected to be an important reaction product, this was not taken into consideration by these investigators. In the absence of a known rate equation, it shall first be postulated that the rate of acetylene formation is also first order with respect to hydrogen, then the rate equation will be tested against available data. The general rate equation for acetylene formation

$$2\,C + H_2 \underset{k_2'}{\overset{k_2}{\rightleftharpoons}} C_2H_2 \tag{6}$$

is

$$\frac{d\,n_{C_2H_2}}{dt} = k_2 S \left(C_{H_2} - \frac{C_{C_2H_2}}{K_2}\right) \tag{7}$$

where

$$K_2 = \frac{k_2}{k_2'} = \left(\frac{C_{C_2H_2}}{C_{H_2}}\right)_{equil.} \tag{8}$$

CONFIDENTIAL
RESTRICTED DATA
Atomic Energy Act - 1954

Testing The Rate Equations

For the following conditions:

a) ideal gas behavior,

b) small gross-surface areas, i. e. small test samples or near the inlet of a tubular chemical reactor, and

c) the equilibrium constants are large compared to the mole fraction reaction product,

It can be shown (as derived in Appendix I) that Equations (3) and (7) reduce to the simplified forms

$$\frac{d\,n_{CH_4}}{dt} = \frac{k_1 S P^*}{R T_G} \tag{9}$$

and

$$\frac{d\,n_{C_2H_2}}{dt} = \frac{k_2 S P}{R T_G} \tag{10}$$

Neglecting the effects of erosion as a first approximation, the rate of graphite corrosion (or surface regression) in mils per minute, r, can be given by the equation

*Note: The order of the rate equation is determined by the exponent on the pressure. By plotting the logarithm of the initial rate versus the logarithm of the pressure, Hedden obtained a unit slope, thus verifying the validity of the first order equation.

CONFIDENTIAL
RESTRICTED DATA
Atomic Energy Act - 1954

$$r = \frac{618\ P}{T_G}\ (k_1 + 2k_2) = \frac{618\ PK}{T_G} \tag{11}$$

where

$$K = k_1 + 2k_2 = \frac{r\,T_G}{618\ P} \tag{12}$$

can be considered an overall, pseudo reaction velocity constant. From basic chemical principles, it is known that the reaction velocity constant is an exponential function of the temperature, i.e., the Arhenius relationship:

$$k = \gamma\ e^{-\Delta H/RT} \tag{13}$$

where γ is a frequency factor, and ΔH is the activation energy. Hence, if the rate equations postulated are correct, a plot of $\ln K$ versus $\frac{1}{T}$ should yield a continuous curve, giving straight line correlations in the limit of predominantly acetylene formation at high temperatures and predominantly methane formation at low temperatures. To test this, values of K were calculated from data taken under conditions that satisfy those listed above. The data, for unfueled graphite, were obtained from the following sources:

1) Landahl[5] - a) isothermal corrosion studies on small coupons of various types of graphite, b) uncoated graphite support block, c) graphite annulus, and

2) Rogers and Sesonske[4] - data taken near the inlet of a tubular graphite reactor.

The data in 1-a, 1-b and 2 were taken from small samples or from near the inlet of a tubular reactor. The data in 1-c were taken under conditions that produced primarily methane and such that the equilibrium constants were large compared to the mole fractions acetylene. It is apparent that these conditions conform to those stipulated in the derivation of Equation (12).

The results are shown in Figure 4. It is clear from this figure that aside from the two low temperature data points for pyrographite, there is no appreciable scatter among the data. In the limit of low temperatures, it appears that the data may be fitted to a straight line with an activation energy of 48,900 BTU/lb-mole or 27.2 kcal/gm-mole. The high temperature data were taken under conditions which produced primarily acetylene, and the data suggest that the acetylene reaction has a higher activation energy. The tentative straight-line Arhenius correlations for the reaction velocity constants k_1 and k_2 are shown as dotted lines. The activation energy for the acetylene reaction is calculated to be 88,000 BTU/lb-mole or 48.9 kcal/gm-mole.

The data of Hedden[1] was not used in the above correlations because Hedden carried out his study in a packed bed of graphite particles with an unknown surface area. The packed bed was relatively long so that the observed reaction rates in the bed represent average values as the effect of concentration changes cannot be evaluated. Nevertheless, the relative reaction rates at the wide range of pressures studied do provide a valid correlation on the order of the reaction. While Hedden's data cannot be used to determine meaningful reaction velocity constants, they can be used to check the reaction velocity correlation developed if the void volume of the packed bed, the flowrates and the surface areas are known. However, the computations required are excessive. In view of the uncertainty of the surface areas and the void volumes, such calculations are not justified. As it will be discussed in a

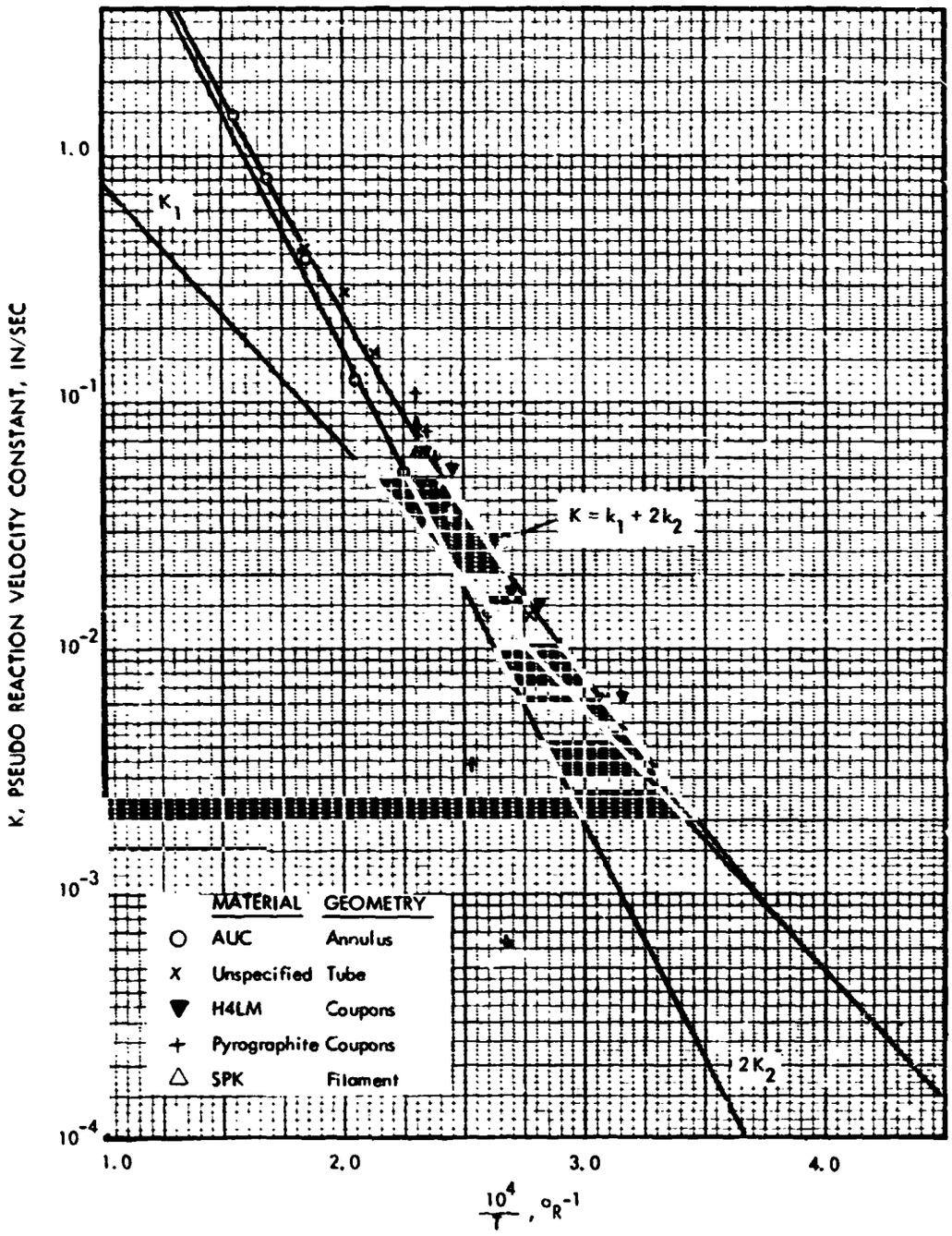

Figure 4

Arhenius Correlation on Apparent Reaction Velocity Constants for First Order Rate Equations

later section, data from more simple flow systems such as straight tubular and annular channels shall be used for independent checks on the correlation.

Rogers and Sesonske's data on TS-34 graphite also could not be used because the pressure level and the inlet methane concentrations are unknown. For example, if the inlet gas is initially saturated with methane, then corrosion would be due to acetylene reactions only, and Equation (12) cannot be used to calculate the apparent reaction velocity constants. This and another special case shall be discussed in a subsequent section.

To test further the validity of the postulated rate equations, and to ascertain the activation energies, values of K were calculated for corrosion data obtained from uranium oxide-fueled graphites. The results are compared with those for unfueled graphite in Figure 5. It is evident from this comparison that, except for the data at the lowest fuel loading, there appears to be a correlation between the frequency factor and the amount of fuel loading; the same activation energy appears to hold for both fueled and non-fueled graphite. At 4000°R a relatively abrupt change in the slope as well as the frequency factor can be observed. This may be due to the fact that at this temperature, there is a change from predominantly methane formation to predominantly acetylene formation. It is readily seen that the increased slope at this point is in good agreement with the slope for k_2 (acetylene reaction) determined from unfueled graphite.

Further Verification of the Correlations

Note that the values of K plotted on Figures 4 and 5 were calculated from Equation (12), which was derived on the assumptions that the equilibrium constants are large compared to the mole fractions. These assumptions and the treatment of data is generally valid for

CONFIDENTIAL
RESTRICTED DATA

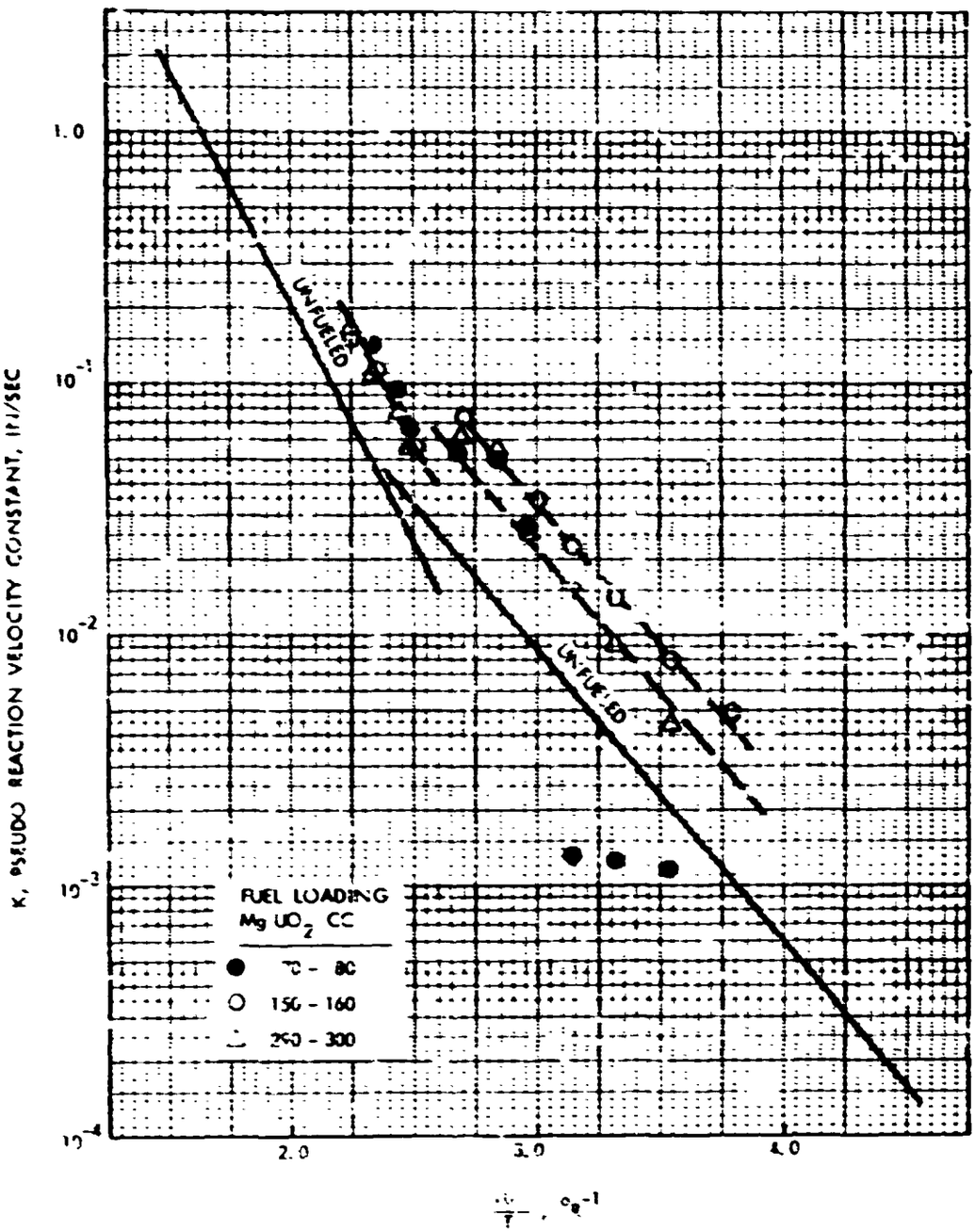

Figure 5

Effect of Fuel Loading on Reaction Constants

CONFIDENTIAL
RESTRICTED DATA

1) high temperatures ($T > 3800^{\circ}R$) and all pressures, and

2) low temperatures ($T < 3800^{\circ}R$) and high pressures.

A more general equation is the following:

$$r = \frac{618\,P}{T_G}\left[k_1\left(1 - \frac{y_1}{K_1}\right) + 2\,k_2\left(1 - \frac{y_2}{K_2}\right)\right] \tag{14}$$

Note that K_2, the equilibrium constant for acetylene increases rapidly with temperature, so that it is generally always significantly greater that y_2. But at low temperatures ($T < 3800^{\circ}R$) and low pressures, values of K_1, the equilibrium constant for methane in terms of mole fractions, becomes small and approaches y_1 if the flowrates were low or if the inlet gas is saturated with methane. Under these specific conditions, Equation (12) does not apply; the first term in Equation (14) becomes negligible compared to the second term, and it can be simplified to

$$r = \frac{618\,P}{T_G}\left[2\,k_2\left(1 - \frac{y_2}{K_2}\right)\right]$$

or

$$2\,k_2 = \frac{r\,T_G}{618\,P\left(1 - \frac{y_2}{K_2}\right)} \tag{15}$$

Now if the fluid velocity is relatively high, $\frac{y_2}{K_2}$ becomes negligible and Equation (15) reduces to

$$2\,k_2 = \frac{r\,T_G}{618\,P}$$

These particular conditions are satisfied by the recent data of Sanders,[13] who studied the corrosion of a single graphite sphere. The values of $2\,k_2$ calculated by Equation (15) for this set of data are compared in Figure 6 with those computed from data taken at high pressures (Figure 4). Excellent agreement is evident.

The data of Gulbransen et. al.[2] were also taken under these general conditions. However, as it was pointed out earlier, complicating side reactions occurred in the test system used. Nevertheless their results were calculated according to Equation (15) and are also shown in Figure 6 for a qualitative comparison. Note that the side reactions are expected to produce CO and CO_2 among other products. Since these reactions corrode graphite in addition to the hydrogenation reactions, the overall weight loss would be greater than that due to hydrogen corrosion alone; hence, as anticipated, the calculated apparent reaction velocity constants are greater than the actual values of k_2. That this is true is evident from Figure 6. The somewhat different slopes observed may be attributed to the fact that the activation energies for the oxidation reactions are different than those of the hydrogenation reactions.

CONFIDENTIAL
RESTRICTED DATA
Atomic Energy Act - 1954

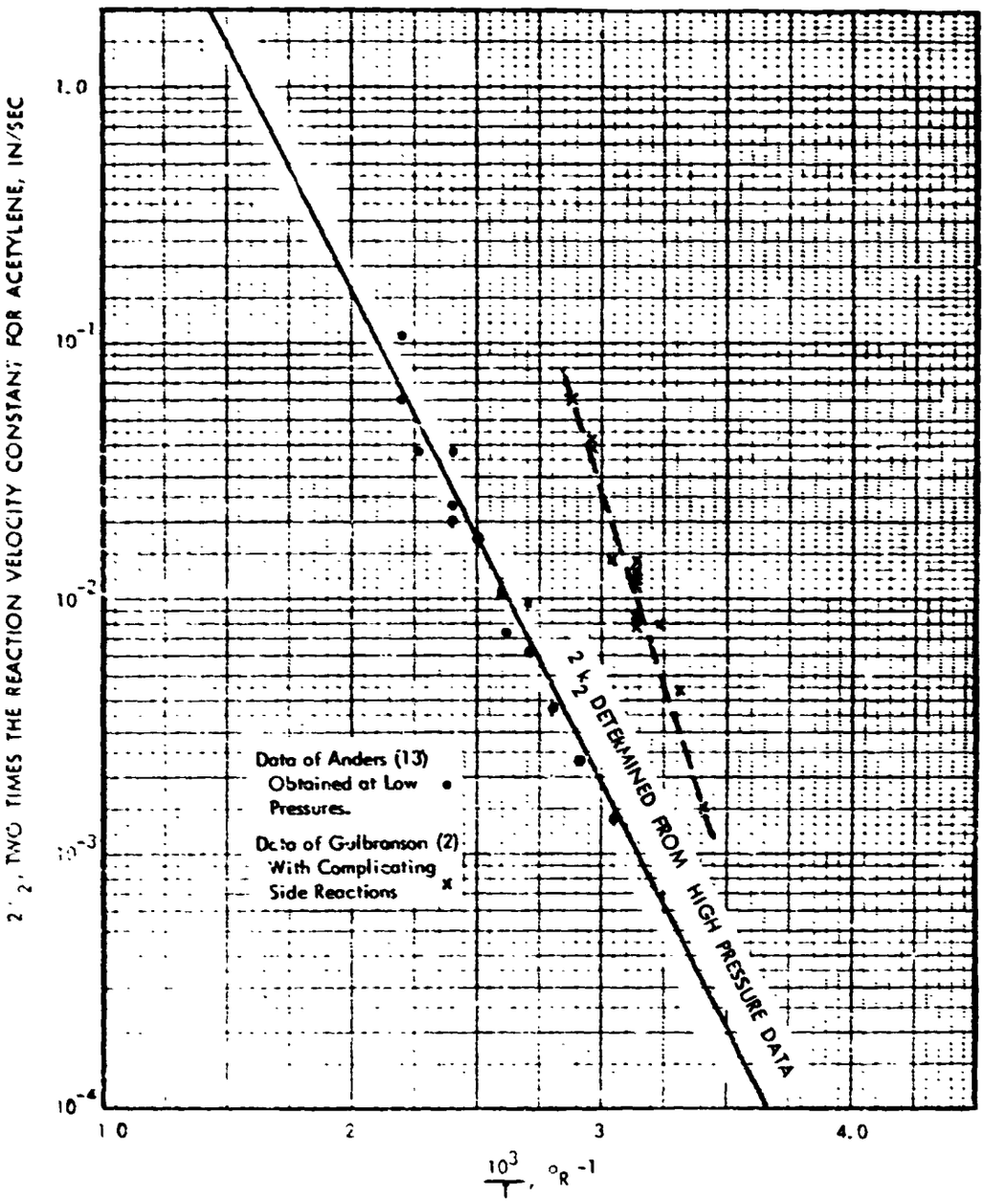

Figure 6

Comparison of Reaction Velocity Constants Calculated From High and Low Pressure Data

CONFIDENTIAL
RESTRICTED DATA
Atomic Energy Act - 1954

It is evident from the significant correlations obtained in Figures 4, 5 and 6 that the first order rate equations postulated are applicable and the same activation energies hold for the following types of graphite: AUC, ATJ, H4LM, SPK, UO_2-fueled and unfueled graphites. In view of this fact and that the data for fueled graphites were taken at considerably lower temperatures, the reaction velocity constants for the methane reaction can be extrapolated with confidence to lower temperatures by the use of the Arhenius relationship and an activation energy of 29.4 kcal/gm-mole.

Since the pseudo reaction velocity constants were calculated from wall regression data, the apparent frequency factors may not be those for the reaction velocity constants of the chemical reactions. To determine the true frequency factors, the effects of erosion and surface effects on overall corrosion must be evaluated.

In general, erosion is expected to be a function of the fluid velocity, surface conditions, and the amount of non-reactive materials present in the graphite. The effects of these factors shall be analyzed.

EFFECT OF PHYSICAL AND CHEMICAL EROSION ON OVERALL CORROSION OF GRAPHITE

Effect of Fuel Loading on Corrosion

The effect of the presence of non-reactive materials on the overall corrosion of graphite appears during the corrosion of fueled materials. A comparison of the K values (Figure 5) for fueled and unfueled graphites clearly showed that the activation energy is the same for both, but the frequency factor increases with increasing fuel loading. This is not surprising, because the presence of non-reacting (with hydrogen) uranium fuel particles contributes to the overall loss of material. Since the K values were calculated from wall regression data, it follows that these should give higher values than those of unfueled graphite.

In the absence of flow, the contribution of fuel loading to overall wall regression can be evaluated as follows:

Let ℓ be the fuel loading in gm of fuel per cc of fueled graphite, ρ the specific gravity of the graphite matrix, s the specific gravity of the fuel compound, then in one cc of the fueled graphite, there is ℓ gm of fuel, and $\rho(1 - \ell/s)$ gm of graphite. It follows that if $\rho(1 - \ell/s)$ gm of graphite is removed by chemical corrosion, ℓ gm of material would be removed by erosion. The ratio of weight eroded to weight chemically corroded shall be denoted by β. This ratio is a function of the fuel loading as given by the relationship

$$\beta = \frac{\ell}{\rho\left(1 - \frac{\ell}{s}\right)} \tag{16}$$

It becomes apparent that from the standpoint of physical erosion alone, fueled graphite would have a higher corrosion rate than that of the unfueled.

The data shown in Figures 4 and 5 were taken with mass velocities ranging from .07 to .80, yet there is no appreciable scatter among the data for unfueled graphite. Moreover, Gulbranson observed no significant difference in corrosion between flow and static systems. Consequently, it may be concluded that in the range of flowrates of interest in the NERVA reactor, erosion of unfueled graphite has no significant effect on the overall corrosion. Thus, the straight lines drawn through the data in Figures 3 and 4 represent the average reaction velocity constants obtained from the data.

In the case of fueled graphite, it shall be postulated that the local rate of erosion is proportional to the local rate of corrosion, fuel loading, and mass velocity.

$$r_e = \alpha G \beta \; r_c \tag{17}$$

But the total rate of corrosion is the sum of chemical corrosion and erosion

$$r_T = r_c + \alpha \beta G r_c$$

$$= r_c (1 + \alpha \beta G) \tag{18}$$

or

$$\frac{\gamma_T}{\gamma_c} = \frac{r_T}{r_c} = 1 + \alpha \beta G \tag{19}$$

From corrosion data obtained near the entrance of UC_2- fueled, but uncoated fuel element coolant channels, α was determined to be 47.5 (β = .214, G = .295). Hence,

$$\frac{k}{k_c} = \frac{\gamma_T}{\gamma_c} = 1 + 47.5 \; \beta G \tag{20}$$

where G is given in lb/in^2-sec.

The data obtained by Landahl on UO_2-fueled graphite coupons could not be used to calculate the constant, α, because the cross-sectional area of the graphite duct in which the coupons were held is unknown.

In view of the fact that very limited data were available for the determination of the constant, α, Equation (20) must not be used for extrapolation to flowrates and fuel loadings considerably beyond those studied.

From the preceding analyses, the following important observations may be made:

1) Neglecting erosion effects, the corrosion behavior of all graphite materials (with the exception of pyrographite) appears to be the same.

2) Erosion does not have a significant effect on the corrosion of unfueled graphite.

3) Erosion has an appreciable effect on the corrosion of fueled graphite; the overall corrosion increasing with increasing fuel loading.

4) The methane reaction has an activation energy of 27.2 kcal/gm-mole.

5) The acetylene reaction has an activation energy of 48.9 kcal/gm-mole.

Corrosion of Pyrographite

The pyrographite data presented in Figure 4 was based on corrosion in the direction normal to the basal plane, "C" direction. The unique structure of pyrolytic graphite is well known. If it is considered that the first in a series of steps leading to hydrogenation of graphite occurs as an attack on the exposed edges of the graphite lattice (as proposed by Zielke and Gorin), then it may be expected that for the corrosion of pyrolytic graphite, this first step, rather than a surface reaction step, is rate controlling. This is due to the fact that the densely packed crystallites in pyrolytic graphite present a minimum of exposed lattice edges. However, if hydrogen flow is parallel to the surface, or if surface defects exist, the lamellar structure may present as many exposed lattice edges per unit gross surface area as ordinary graphite. This seems to be suggested by the fact that at relatively low temperatures, the apparent reaction velocity constants (K) calculated are significantly lower than those of the other graphites (see Figure 4). However, at higher temperatures, the K values are the same as those for normal graphites. It may be assumed that at higher temperatures

the surface is attacked more readily, thus exposing subsequent layers and larger surface areas. Moreover, hydrogen may flow between the layers, thus increasing the effective reaction surface areas. The data available are inadequate for the determination of the specific reaction velocity constants. However, those presented in Figure 4 suggest that at temperatures greater than 4000°R, the reaction velocity constant equation for normal graphites may be used for pyrolytic graphite also.

HYDROGEN CORROSION OF GRAPHITE COMPONENTS

As independent and critical checks on the validity of the rate equations developed and the reaction velocity correlations, the local corrosion rates and/or the overall weight losses were predicted from known geometries, flowrates, temperature and pressure distributions for those sets of component test data that include these information. These data are described in detail below.

Unfueled Elements

A number of experimental tests were carried out at LASL on approximately 12-inch long, unloaded elements in an attempt to study the effect of pressures and flowrates on the corrosion of graphite. The data are reproduced in Table II. These tests were carried out under isothermal conditions, and the gas was preheated by passing through an electrically-heated, coated element mounted upstream of the test piece. Post test examination of the test specimens showed fairly uniform corrosion both axially and among the 19-holes. This essentially verified the existence of isothermal conditions. The solution of the flow reactor equation is given in Appendix II. The flow equation was first integrated to give the axial distribution of the hydrocarbon concentrations. From this, the local graphite wall regression distribution was calculated. Finally, this was integrated to give the total weight change for the test piece. The calculated weight losses are compared with the observed values in Figure 7. It is apparent that the calculated values are on the average lower than

CONFIDENTIAL
RESTRICTED DATA
Atomic Energy Act - 1954

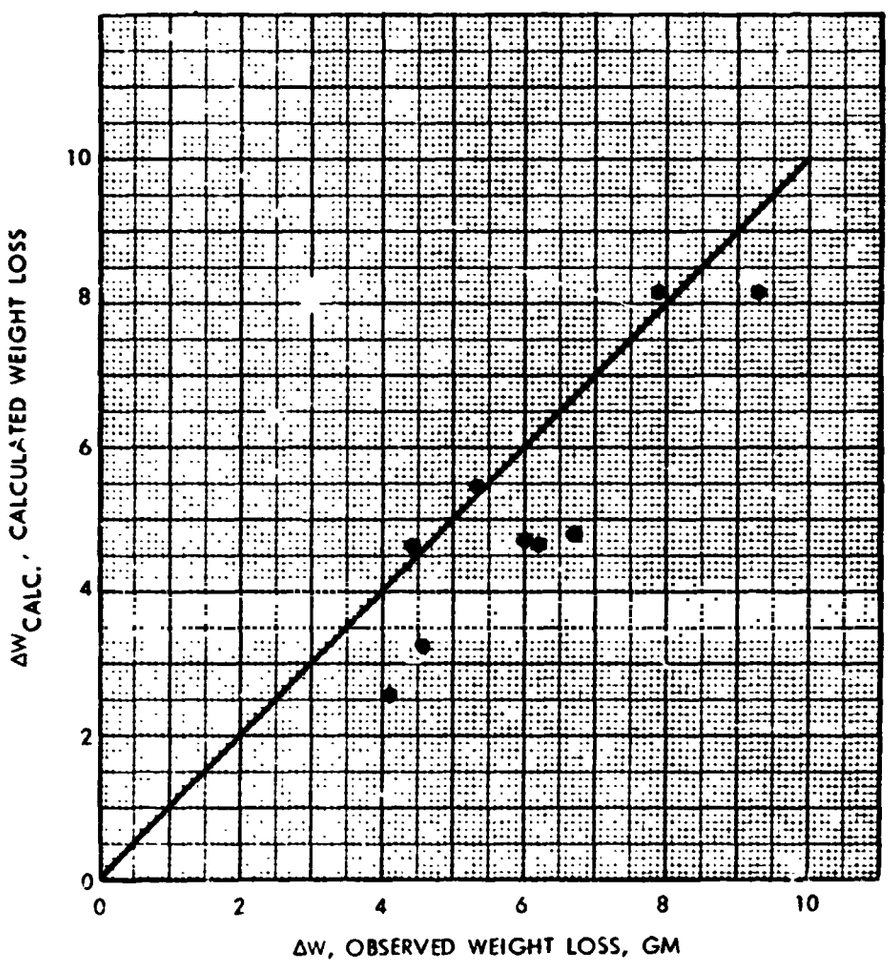

Figure 7

Comparison of Observed and Calculated Overall Weight Loss - 19-Hole Uncoated and Unfueled Elements

CONFIDENTIAL
RESTRICTED DATA
Atomic Energy Act - 1954

those observed. The average deviation is 12.5%. The lower calculated corrosion weight loss is probably due to the fact that erosion effects had been neglected. Consequently, the agreement between observed and calculated data can be considered to be fairly good. In view of the fact that the data were taken over a wide range of pressures (300-1000 psia), this provides further evidence on the validity of the first order rate equations postulated.

AUC - Graphite Annulus

Hydrogen corrosion in cracks, gaps, and slots had been studied by Landahl;[5] however, only one complete set of data was taken. The study was carried out in a 60-inch long graphite annulus (AUC graphite) with an I.D. of 1.125-inches and an annular gap of .01-inches. The local temperature and the wall regression were experimentally measured and the data are given in Table II.

With the known geometry, flowrate, upstream pressure, and the temperature distribution, the pressure distribution was first calculated. A step-wise integration of the flow equation was then carried out to calculate the local dynamic methene and acetylene concentrations. The procedures are discussed in Appendix III. Finally, the local corrosion rates were calculated from the equation

$$\frac{dr}{dt} = \frac{618\,P}{T_G}\left[k_1\left(1 - \frac{y_1}{K_1}\right) + 2k_2\left(1 - \frac{y_2}{K_2}\right)\right] \qquad (21)$$

The calculated local corrosion rates are compared with the observed values in Figure 8. The excellent agreement between observed and calculated local corrosion rates provide further evidence on the validity of the rate equations postulated and the reaction velocity constants used.

CONFIDENTIAL
RESTRICTED DATA
Atomic Energy Act - 1954

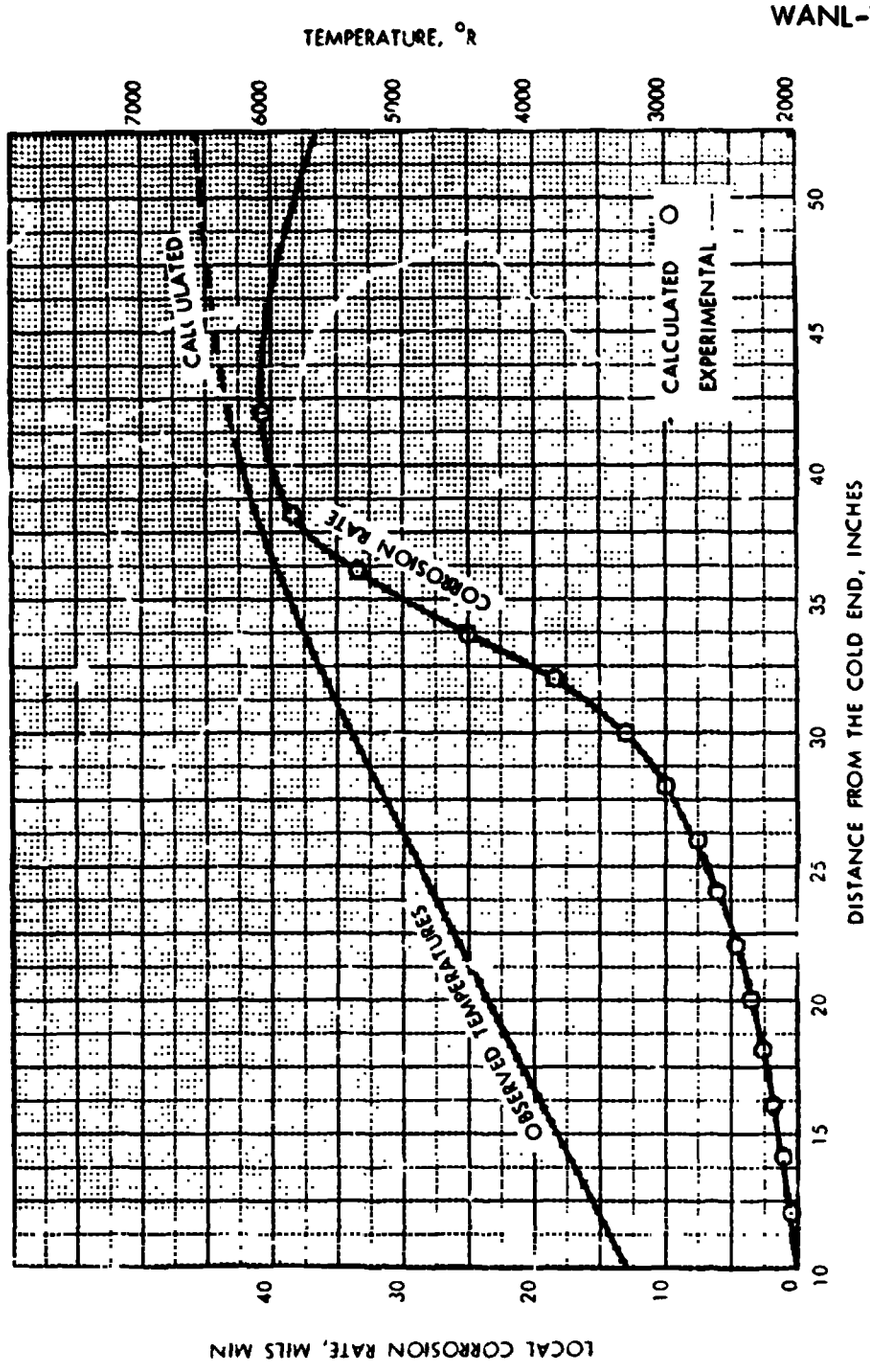

Figure 8

Comparison of Calculated and Experimental
Local Corrosion Rates AUC Graphite Annulus - .010 Inch Gap

CONFIDENTIAL
RESTRICTED DATA
Atomic Energy Act - 1954

Uncoated Coolant Channels

During environmental testing of NRX-A2 fuel elements, it was found that one element had two coolant channels that were predominantly uncoated. Channel 3 was found to be uncoated up to approximately 42-inches and Channel 1 was uncoated up to 34-inches. The local corrosion rates were measured and the results are given in Table III. The total measured weight loss for the element was 30.7 gm.

Since the temperature, pressure, and flow distributions for this test can be readily calculated, this data can provide an excellent check on the validity of the rate equations proposed and the correlations for the reaction velocity constants.

Details on the computational procedure are given in Appendix IV. The calculated local corrosion rates are compared with the observed values in Figure 9. The calculations were based on average flowrates and average material temperatures (between the maximum internal and the surface temperatures). The pressure and temperature distributions used are given in Appendix IV.

It is evident from Figure 9 that there is good agreement between the observed and calculated corrosion rates. An integration of the local corrosion along the coolant channels gave a total weight loss of 33.0 gm, which is also in good agreement with the experimental value of 30.7 gm. The somewhat higher calculated value may be due to the uncertainty of the exact lengths of the uncoated portions of the coolant channels.

Center Hex Corrosion

During the environmental testing of a single cluster in the A-10 furnace, severe corrosion was observed on the center hex.[7] Corrosion occurred on the graphite surface, facing the Berlox insulator sleeve. The graphite surface was exposed to hydrogen flowing axially down the annulus. Local corrosion measurements gave a

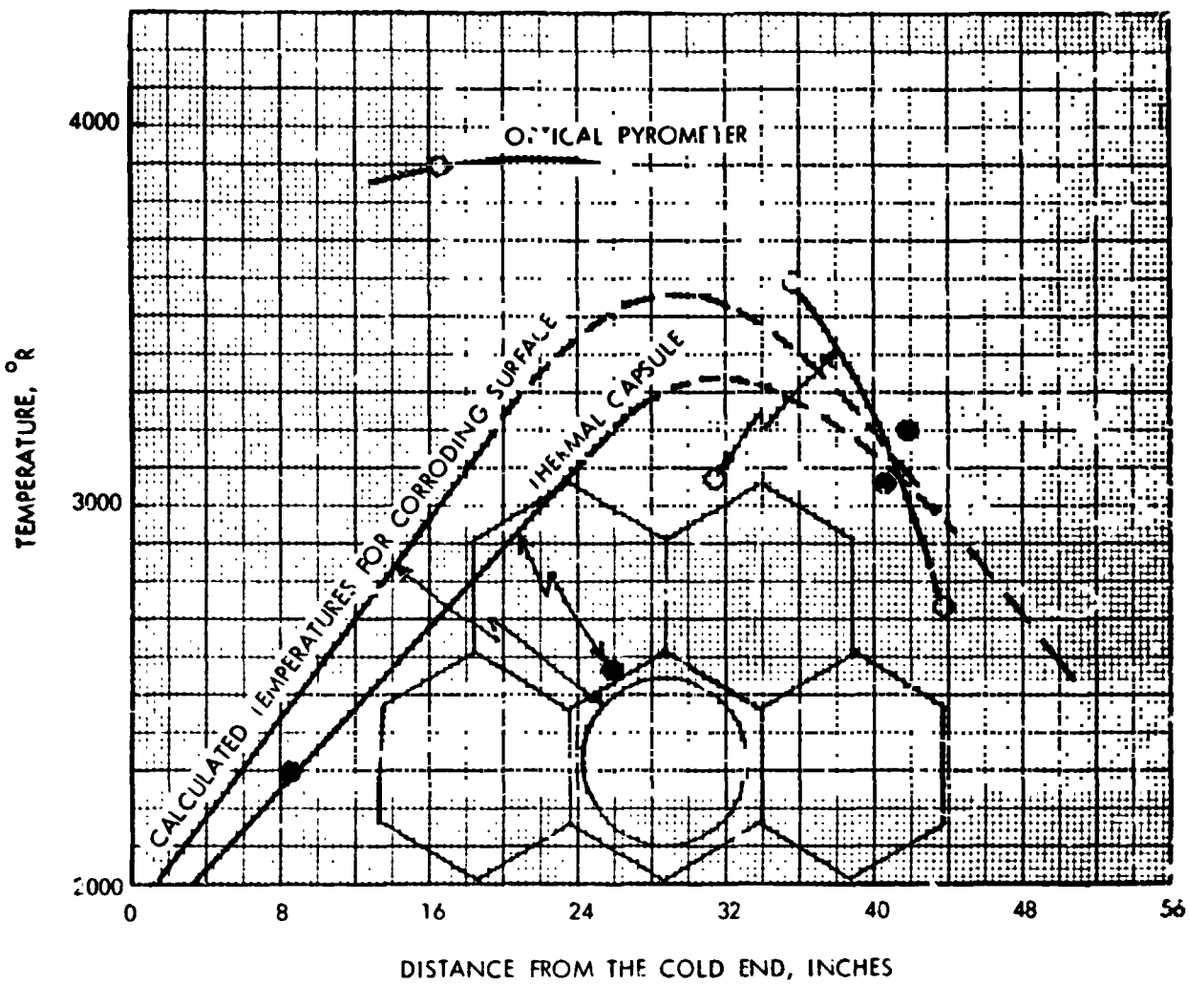

Figure 9

Comparison of Observed and Calculated Local Corrosion Rates
Uncoated, NRX-A2 Type Fueled Coolant Channels - A-2 Furnace Run 331

regression profile which showed a gradual increase to a maximum at 22-inches from the inlet and then decreased rapidly with increasing distance. Although the flowrate is unknown, limited temperature measurements were made with thermal capsules at a position shown in Figure 10.

Near the inlet, the methane concentration must be negligible. Since the inlet pressure is known and it did not decrease appreciably for short distances, the graphite wall temperatures were calculated from the local corrosion measurements by the equation

$$r = \frac{618\ k_1\ P}{T_G} \text{ mils per minute} \tag{22}$$

where k_1 is a function of the wall temperature. For a good approximation, it was assumed that $T_G = T_w$ and the wall temperatures were determined from the relationship

$$\frac{k_1}{T} = \frac{r}{618\ P} \tag{23}$$

The temperature measurements and calculated values are compared in Figure 10. It is evident that the calculated values are consistently higher than those observed, but it is known that the temperatures at the corroding surfaces are higher than those at which they were measured. This suggests that the thermal capsule temperature measurements were fairly accurate. Thus, using the thermal capsule temperature measurements as a guide, the complete temperature distribution was estimated as shown.

If both the temperature and pressure distributions are fixed, only one flowrate can give the particular corrosion distribution observed. Consequently, the flowrate through the annulus was determined by a trial and error procedure.

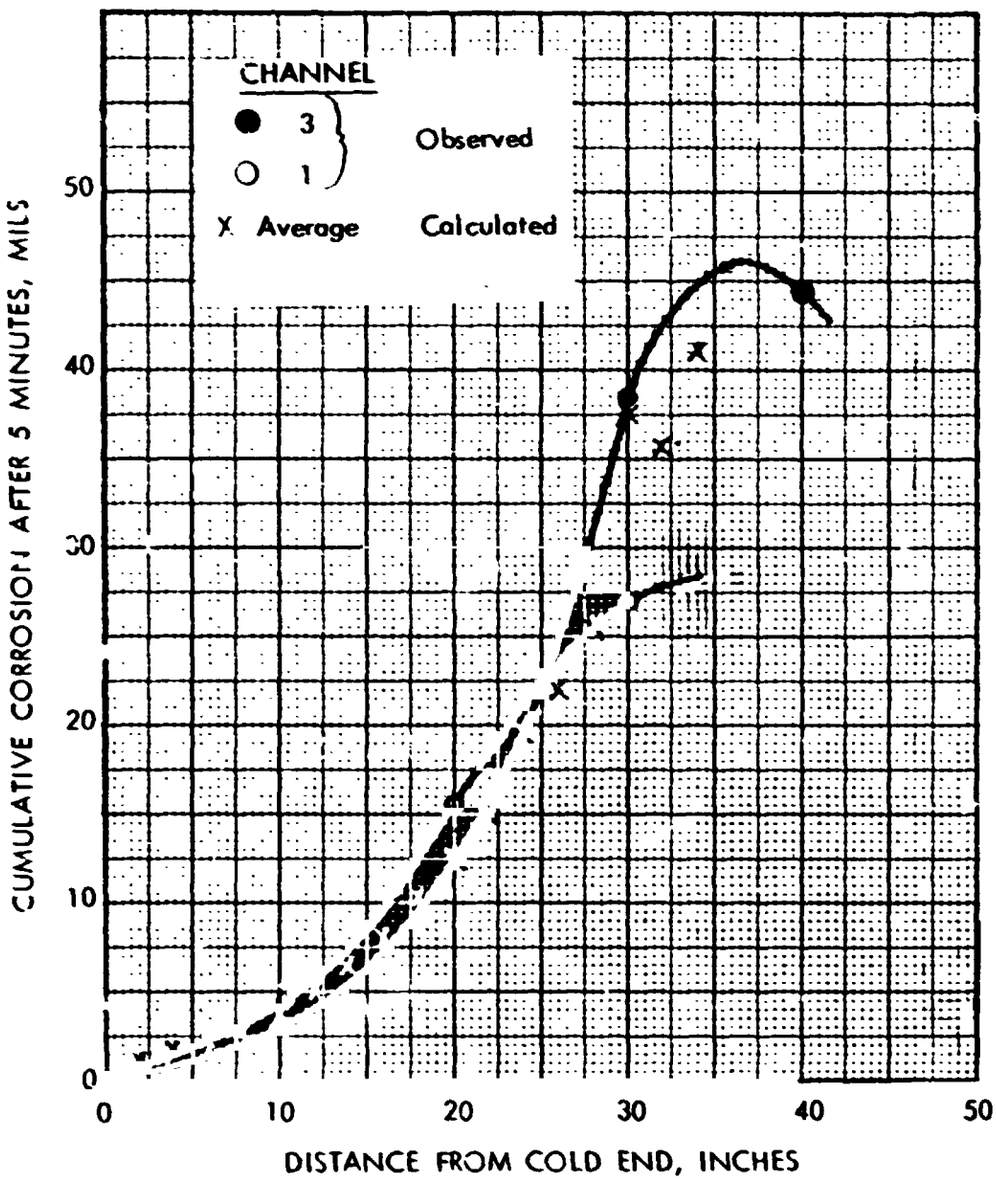

Figure 10

Observed and Calculated Temperatures in the Single Cluster Corrosion Test

The single cluster was operated at near maximum temperature, for a period of 35 minutes. During this period, the pressure drop decreased from 55 to 20 psi, and the total hydrogen flowrate varied from 150 to 212 scfm. For the purpose of the following calculations, an average pressure drop was assumed. The calculations were carried out as follows:

1) assume a flowrate.

2) calculate the pressure distribution.

3) calculate the corrosion distribution. If the results agree with that observed, then the assumed flowrate is correct. If it is not, repeat Steps 1 - 3.

Since the wall regression is small compared to the diameter, a constant perimeter was assumed for the calculations. The results for two different flowrates are compared with the observed local corrosions in Figure 11. It is evident from this figure that a flowrate of 1.272×10^{-4} lb/sec (1.38 scfm) through the annulus gives very good agreement between observed and calculated corrosion distributions. The somewhat lower calculated values at the 21 to 25-inch location may be due to errors in the temperatures estimated for this region.

DISCUSSIONS

Corrosion Measurements as Aid to Analysis

From the examples given on the analysis of corrosion, it has been shown that, given the correct rate equations and reaction velocity constants, local corrosion in a flow system is a function of

1) the temperature distribution,

2) the pressure distribution,

3) flowrate,

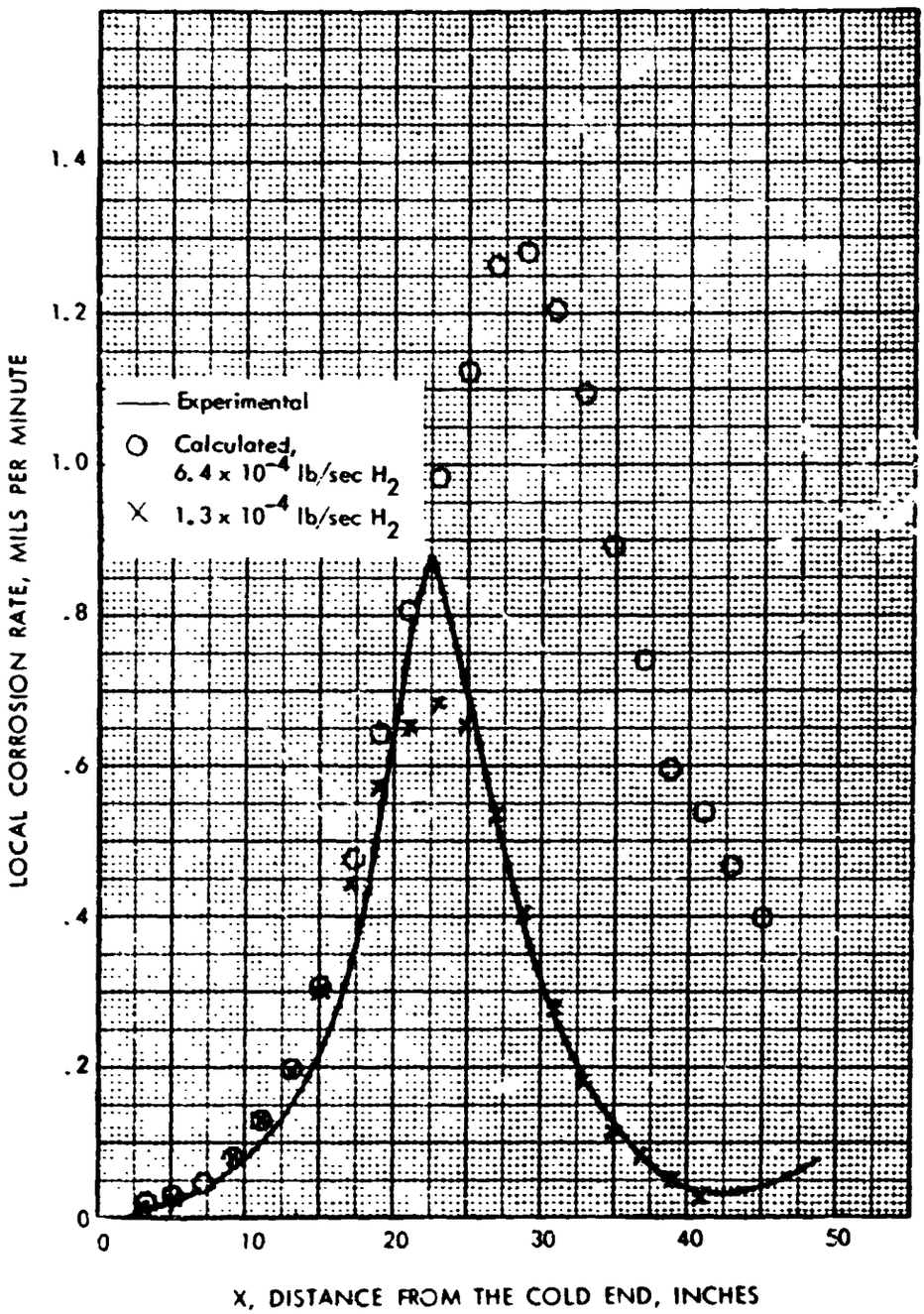

Figure 11

Comparison of Observed and Calculated Center Hex Corrosion (Graphite Annulus)

4) reaction surface area distribution, and

5) initial and/or boundary hydrocarbon product concentrations (in the case of fresh hydrogen flow through a tube or annulus, the product concentrations at the entrance are zero).

It has been demonstrated that, given the above information, local corrosion can be predicted. It has been shown further that if local corrosion measurements are available, any of the five (5) variables can be determined from the corrosion data and the other four (4) known variables. This is demonstrated by the following example.

In the corrosion of the graphite annulus, temperature data were available only up to 45.5-inches from the inlet, whereas local corrosion rates were measured up to 56-inches. In view of the excellent agreement between observed and calculated corrosion rates, the local temperatures beyond 45.5-inches can be determined by extrapolation with the aid of local experimental corrosion data. The results are shown on Figure 8. It is suggested that local corrosion measurements can provide an additional means of temperature determination in NERVA test reactors or component tests, particularly in high temperature regions where available instrumentation are inadequate and unreliable.

Mechanisms of Hydrogenation Reactions

The validity of the first order rate equations for both methane and acetylene formations has been well substantiated from experimental data. However, detailed mechanisms can also be derived to show the first order dependence of the rate equation. For the methane reaction, both Hedden and Zielke and Gorin postulated surface reaction mechanisms from which a first order rate equation can be derived.

CONFIDENTIAL
RESTRICTED DATA
Atomic Energy Act - 1954

For the acetylene formation, it is postulated that the reaction consists of the following steps:

a) $$-\overset{|}{C}=\overset{|}{C}- + H_2 \underset{k_1'}{\overset{k_1}{\rightleftharpoons}} H\overset{|}{C}=\overset{|}{C}H$$

b) $$H\overset{|}{C}=\overset{|}{C}H \underset{k_2'}{\overset{k_2}{\rightleftharpoons}} CH\equiv HC$$

Step (b) is a surface rearrangement step and is expected to be rate-controlling. The first step is assumed rapid; hence, the concentration of C H can be assumed to be at its equilibrium value. The resulting rate equation is then

$$\frac{d\,n_{C_2H_2}}{dt} = k_2 K_o C_o \left(C_{H_2} - \frac{C_{C_2H_2}}{K_2} \right) \tag{24}$$

where C_o, the initial concentration of active sites, is proportional to the gross surface area, S. A derivation of Equation (24) is given in Appendix V. Lumping all the constants into one yields

$$\frac{d\,n_{C_2H_2}}{dt} = k_2 S \left(C_{H_2} - \frac{C_{C_2H_2}}{K_2} \right) \tag{25}$$

which is identical to Equation (7).

It has been shown that the mechanisms of methane and acetylene reactions may be attributed to rate controlling steps that follow the same initial step in which

CONFIDENTIAL
RESTRICTED DATA
Atomic Energy Act - 1954

a single carbon bond is hydrogenated. Since this first step is fast and methane and acetylene are formed by succeeding parallel steps, the additive contribution of the reactions to the corrosion of graphite is therefore valid. This can be summarized by the following steps:

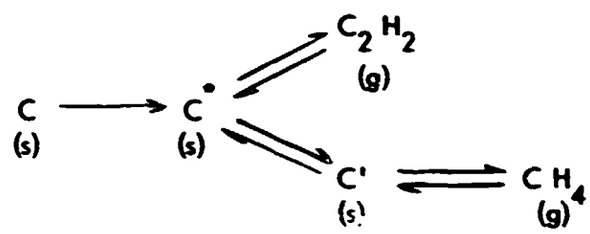

Both acetylene and methane formations are functions of the surface complex C,* which is in turn a function of the gross surface area.

It must be pointed out that the effects of chemical reaction and erosion were deduced from overall graphite surface regression data. It is obvious that for a more rigorous study on the kinetics of the chemical reactions, the effects of chemical reaction and erosion must be studied separately, and instantaneous reaction data would be required. However, in view of the fact that the effective gross reacting surface area may vary from material to material and that it cannot be measured or rigorously defined, such an approach will prove most difficult.

It is important to note that following Hedden, the basic rate equations were written in terms of concentrations. It is equally permissible to write the rates of methane and acetylene formations in terms of partial pressures, i. e.

$$\frac{d\,n_{CH_4}}{dt} = k_1 S \left(P_{H_2} - \frac{P_{CH_4}}{K_p P_{H_2}} \right) \tag{26}$$

From which one can obtain the simplified equation

$$\frac{d\,n_{CH_4}}{dt} = k_1 S P \left(1 - \frac{y_{CH_4}}{K_y} \right) \tag{27}$$

Note that the general form of the rate equation is retained, but the denominator now does not have a temperature. Consequently, the calculated reaction velocity constants would give different values and different units. Either Equation (25) or (26) could have been used, and the first was chosen merely because the resulting reaction velocity constant gives units in terms of inches per second, which is analogous, but by no means equal, to the rate of surface regression.

The detailed mechanisms postulated here were based on the assumption that surface reaction is rate-controlling. This was generally assumed by all previous investigators.[1,2,3,4] That this mechanism is consistent with the assumption that corrosion is based on the gross external surface area can be seen as follows: Graphite is known to be a relatively porous material, possessing large pore surface areas. However, if the rate of pore diffusion is significantly slower than the rate of surface reaction, then the gas within the pores would be saturated with hydrocarbons; consequently, no significant reactions can take place in the pores. The hydrogen-graphite reaction continuously removes the solid material, thus exposing fresh surface active sites. This phenomenon suggests that

1) the rate of surface reaction is slower than the rate of pore diffusion, and
2) the total surface active sites available for reaction, hence the gross external surface area, is approximately a constant.

These phenomena have been well substantiated by the successful correlation of the data. The internal pore surface areas are known to be many times greater than the gross external surface areas. Moreover, they vary with the density and porosity of the graphite material. Hence, if the rate of hydrogen-graphite reaction is controlled by pore diffusion, a significant correlation could not have been obtained among the different graphite materials.

Rates of Bulk Diffusion and Pore Diffusion

Most of the data treated here were taken at relatively high flowrates where the resistance to turbulent mass transfer is negligible. However, in many practical situations such as occurs during interstitial flow in the NERVA reactor, hydrogen flow is essentially laminar. In this case, it is necessary to know whether surface reaction is still rate-controlling or whether the resistance to diffusion has increased appreciably so that the surface rate-controlling mechanism becomes invalid. A detailed analysis of the diffusion phenomenon is treated in Appendix VI. A comparison of calculated rates of diffusion versus the apparent rates of reaction shows that the rate of bulk diffusion is thousands of times greater than the apparent rate of reaction and the rate of Knudsen diffusion is hundreds of times greater than the apparent rate of reaction. These facts provide further evidence that surface reaction is the rate controlling process.

It should be pointed out here that since surface reaction is rate-controlling and resistance to mass transfer is negligible, the surface temperature may be used instead of the bulk temperature throughout the rate equations.

Carbon Deposition

As discussed in the Appendix, a straight-forward step-wise integration procedure was used to calculate local methane and acetylene concentrations and then

the local corrosion rates. Although this procedure has been useful for the conditions calculated, it can be readily shown that this does not permit the prediction of carbon deposition, i. e. the reverse reaction. To compensate for this deficiency, it is only necessary to check the local ratio of mole fraction methane to the equilibrium constant, y_1/K_1. When this value approaches one, then an iteration procedure can be used to calculate the local methane concentrations. Consequently, for general purpose calculations, a computer solution is recommended.

For the acetylene reaction, y_2/K_2 is generally less than one. This indicates that carbon deposition does not occur in the acetylene reaction. This fact clearly suggests that corrosion due to the acetylene reaction is potentially more serious if the reactor attains temperatures greater than those encountered at the present.

Effect of Radiation

Corney and Thomas[11] studied the effects of pile radiation on the reaction between hydrogen and graphite. The results show that at a pressure of 30 psia and a temperature of 1360°R, the rate of reaction forming methane is 10 times greater with radiation than without, but at 1540°R, it is only 4.4 times greater. The trend suggests that at the considerably higher temperatures encountered in the reactor, radiation may have a negligible effect on the rate of corrosion. This seems to be borne out by limited data obtained at higher temperatures by LASL.[12]

Heats of Reaction

It is known[14] that methane and acetylene formations are exothermic reactions, giving 32,200 BTU/lb-mole CH_4 and 54,000 BTU/lb-mole C_2H_2. In the experimental studies analyzed here, the temperatures were controlled, and the hydrogen flowrates were large. For these conditions, the heat of reaction can be neglected. However, it is conceivable that the heat of reaction may be important

under special conditions in which the heat input is held constant and corrosion is significant. If such a situation arises, the heats of reaction must be included in the analysis.

Maximum Local Rate of Corrosion

The general equation for the local rate of corrosion is given by Equation 14. In many cases of practical interest, the local methane and acetylene concentrations are negligible and/or the ratios y_1/K_1 and y_2/K_2 in Equation 14 are negligible compared to one. This implies that the reverse reactions are negligible. In these instances, the local rate of corrosion approach the maximum theoretical value given by the general equation

$$r = \frac{618}{T}(1 + 47.5\,\beta\,G)\,KP\ \frac{\text{mils}}{\text{min}}$$

where β is a function of the fuel loading as given by Equation 16, G is the mass velocity in lb/in^2-sec, and K is defined by Equation 12.

Typical cases where maximum corrosion rate is approached are the following:

1) Flow inlet regions

2) Fuel element coolant channels where cracks in the niobium carbide coating exist. Such instances, resulting from thermal stresses, caused a number of aborted tests during fuel element testing in the A-2 furnace.

3) Core peripheral corrosion near the hot end, where acetylene deficient hydrogen comes into contact with hot surfaces.

4) Any location where small areas of graphite are exposed to relatively large amounts of fresh hydrogen.

An analysis of specific cases will be presented in a later report.

Recommended Experimental Studies

From the experimental data obtained at LASL on UO_2-fueled graphite coupons, it was shown that the amount of fuel loading has a significant effect on the erosion of the material. However, NERVA fuel elements are currently made with UC_2 fuel beads, and well-controlled experimental corrosion data on the latter material is not available. It is apparent that such data are urgently needed. It is suggested that data can be readily obtained by mounting uncoated fuel element sections in the support block holder of the A-2 furnace.

CONCLUSIONS

From the results of this study, it may be concluded that within the range of temperatures and pressures of concern in the NERVA reactor, both methane and acetylene formations are important reactions contributing to the overall corrosion of graphite. The methane and acetylene reactions can be simply represented by first order rate equations that are proportional to the gross exposed surface area. The activation energy for the methane reaction is 27.2 kcal per gm-mole and that for the acetylene reaction is 48.9 kcal per gm-mole. The specific reaction velocity constants can be given by the equations:

$$k_1 = 8.975 \exp(-48{,}900/RT) \text{ in/sec} \tag{28}$$

and

$$k_2 = 574 \exp(-88{,}000/RT) \text{ in/sec} \tag{29}$$

where: R = 1.9872, and T is in degrees Rankine.

The equations are specifically applicable to ATJ, H4LM, AUC, SPK, and unfueled graphites. For other types of graphite, such as ZTA and Graphitite "G", the same equations are expected to apply, but experimental data should first be obtained before the equations can be used with full confidence on these latter materials. For UC_2-fueled graphite elements, the frequency factors in Equations (28) and (29) should be multiplied by

$$1 + 47.5\,\beta\,G \tag{30}$$

where G is the mass velocity in lb/in^2-sec, and

$$\beta = \frac{\ell}{\rho(1 - \ell/s)}$$

CONFIDENTIAL
RESTRICTED DATA
Atomic Energy Act - 1954

is the UC_2 fuel loading in gm/cc, s is the specific gravity of the fuel, and ρ is the specific gravity of the graphite matrix.

It must be cautioned that in view of the paucity of data on the corrosion of uncoated, UC_2-fueled graphite, Equation (28) must not be extrapolated to mass velocities appreciably beyond that for which data were available, i. e. .295 lb/in^2-sec. Additional data is required to determine the exact nature of erosion and the effect of fuel loading on this phenomenon.

The data correlated in this study were obtained over pressures ranging from .0016 to 1100 psia and at temperatures ranging from 1800°R to 6450°R. Since the correlations obtained covered a variety of graphite materials, the first order rate equations proposed here and the reaction velocity constants developed may be used with confidence for the prediction and analysis of corrosion on graphite materials and reactor components.

The results from the analysis on the rates of bulk and pore diffusion leaves little doubt that surface reaction is the rate-controlling mechanism.

Due to the anistropic nature of pyrographite, the mechanisms of corrosion of this material appears to be quite complex and it is not well understood. Further research is necessary in order to ascertain the differences in corrosion rates between "a" and "c" planes.

CONFIDENTIAL
RESTRICTED DATA
Atomic Energy Act - 1954

ACKNOWLEDGMENTS

The author is indebted to C. E. Landahl of Los Alamos Scientific Laboratory for providing some of the data that had not been published and for a great deal of helpful information and discussions. Thanks are also due Mr. J. D. Rogers of LASL for detailed information on his early work.

CONFIDENTIAL
RESTRICTED DATA
Atomic Energy Act - 1954

NOMENCLATURE

a	a proportionality constant
b	a proportionality constant
C	concentration or corrosion perimeter
G	mass velocity
ΔH	activation energy in Arhenius relationship, consistent units
k	forward reaction velocity constant
k'	reverse reaction velocity constant
K	equilibrium constant or pseudo reaction velocity constant
ℓ	fuel loading, grams fuel per cc fueled graphite
n	number of moles of c component
N	total molar flowrate, lb-moles/second
P	local pressure
r	rate of hydrocarbon formation, or surface regression
R	gas constant in consistent units
s	specific gravity of the uranium fuel compound, gm/cc
S	gross reactive surface area
t	corrosion time, seconds
T	temperature
W	weight
y	mole fraction
Z	axial distance along a flow channel

Subscripts

C	carbon or chemical
CH_4	methane
C_2H_2	acetylene

CONFIDENTIAL
RESTRICTED DATA
Atomic Energy Act - 1954

e	erosion
G	gas
H_2	hydrogen
i	ith reaction
T	total
0	surface active sites
1	methane reaction
2	acetylene reaction

Greek Letters

α	proportionality constant
β	dimensionless fuel loading factor
γ	frequency factor in Arhenius relationship

$$k = \gamma e^{-\Delta H/RT}$$

ρ	specific gravity, gm/cc
τ	total corrosion time

REFERENCES

1. Hedden, K., "The Formation of Methane from Hydrogen and Carbon at High Temperatures and Pressures," Proceedings of the Conference on Carbon, Vol. 1, The McMillan Company, N. Y. 1962, pp. 125-131.

2. Gulbransen, E. A., Andrews, K. F., and Brassart, F. A., "The Reaction of Hydrogen with Graphite at 1200°C to 1650°C," Westinghouse Research Laboratories, Scientific Paper 64-139-120-P2, May 4, 1964.

3. Zielke, C. W. and Gorin, E., "Kinetics of Carbon Gasification," Industrial and Engineering Chemistry, Vol. 47, No. 4, April 1955, pp. 820-823.

4. Rogers, J. D., and Sesonske, A., "Graphite-Hydrogen-Methane Kinetics Above 1600°K," LAMS-2896, May 26, 1963.

5. Landahl, C. E., "Hydrogen Corrosion, Cracks, Gaps, and Slots," LASL internal report N-1-859, March 27, 1963.

6. Landahl, C. E. to Rogers, J. D., "Flow Pressure Correlation Tests with 1-Minute Switchover to Hydrogen," Unpublished data, May 8, 1962.

7. Foster, R. D., and Gilchrist, M. C., "First Single Cluster Corrosion Test WANL Hydrogen Corrosion Test Facility," WANL-TME-1072, March, 1965.

8. Lowrie, R. L. O., "Research on Physical and Chemical Principles Effecting High Temperature Materials for Rocket Nozzles," Quarterly Progress Report, NP12130, Union Carbide Research Institute, September 30, 1962.

9. Data obtained by Fluid Flow Laboratory and Materials, Unpublished.

10. Landahl, C. E., Los Alamos Scientific Laboratory, Private Communications, unpublished data on uncoated ATJ graphite support blocks, presented in Table IV.

11. Corney, N. S., and Thomas, R. B., UK AERE C1-R2502, RCTC/P118, 1958.

12. Zemanick, P. P. and Chi, J. W. H., Trip Report, Trip to LASL, January, 1965.

13. Sanders, William A., "Rates of Hydrogen-Graphite Reaction Between 1550°C and 2260°C," NASA-TND-2738, February, 1965.

14. Hougen, O. A., et. al., "Chemical Process Principles," Part I, John Wiley & Sons, Inc., 1954, p. 304 and p. 311.

15. Bird, R. B., et. al., "Transport Phenomena," John Wiley & Sons, Inc., New York, 1960, p. 507.

16. Nuclear Graphites, Nightingale, R. E., Ed., Academic Press, Inc., New York, 1962, p. 103.

17. Handbook of Physics and Chemistry, 4th Edition, Chemical Rubber Publishing Co., Cleveland, Ohio, 1958, p. 3373.

18. Smith, J. M., Chemical Engineering Kinetics, McGraw-Hill Book Company, New York, 1956, p. 268.

CONFIDENTIAL
RESTRICTED DATA
Atomic Energy Act - 1954

APPENDIX I

Simplifying the Rate Equations

By assuming ideal gas behavior, the rate equations can be written in terms of mole fractions and the total pressure and bulk gas temperatures as follows:*

$$\frac{d\,n_{CH_4}}{dt} = \frac{k_1 S P}{R T_G}\left(1 - y_{CH_4} \quad \frac{y_{CH_4}}{K_1\left[1 - y_{CH_4}\right]}\right) \tag{1}$$

and

$$\frac{d\,n_{C_2H_2}}{dt} = \frac{k_2 S P}{R T_G}\left(1 - y_{C_2H_2} - \frac{y_{C_2H_2}}{K_2}\right) \tag{2}$$

For the conditions at which available experimental data were taken, the equilibrium mole fractions of methane and acetylene are small compared to 1 and Equations (1) and (2) can be simplified to give

$$\frac{d\,n_{CH_4}}{dt} = \frac{k_1 S P}{R T_G}\left(1 - \frac{y_{CH_4}}{K_1}\right) \tag{3}$$

---

*Since the first order rate equation can be attributed to either an adsorption or surface reaction mechanism, this implies that mass transfer from the bulk phase to the gas-solid interface is rapid; whence the interfacial concentrations are equal to the bulk concentrations.

CONFIDENTIAL
RESTRICTED DATA
Atomic Energy Act - 1954

$$\frac{d\,{}^{n}C_2H_2}{dt} = \frac{k_2 SP}{R T_G}\left(1 - \frac{{}^{y}C_2H_2}{K_2}\right) \tag{4}$$

In addition, if the graphite samples or the reaction surfaces are small, or if the hydrogen velocity (in a flow reaction system) is high, the mole fractions of the hydrocarbons are small and the ratio y/K can be neglected; whence, the rate equations can be further simplified to

$$\frac{d\,{}^{n}CH_4}{dt} = \frac{k_1 SP}{R T_G} \tag{5}$$

and

$$\frac{d\,{}^{n}C_2H_2}{dt} = \frac{k_2 SP}{R T_G} \tag{6}$$

If the two reactions are linearly independent, the rate of graphite corrosion in mils per minute, r, can be given as

$$r = \frac{618\,P}{T_G}\;k_1 + 2\,k_2 = \frac{618\,K\,P}{T_G} \tag{7}$$

where

$$K = k_1 + 2\,k_2 = \frac{r\,T_G}{618\,P} \tag{8}$$

can be considered an overall, pseudo reaction velocity constant.

CONFIDENTIAL
RESTRICTED DATA
Atomic Energy Act - 1954

APPENDIX II

Isothermal Corrosion for Short Corrosion Times

The general flow reactor equation, obtained from a mass balance of carbon in the gaseous phase can be written in the form

$$(r_1 + r_2)\ dx = dN\ (y_1 + y_2) \tag{1}$$

where r_1 is the rate of methane formation

r_2 is the rate of acetylene formation

y_1 and y_2 are the mole fractions methane and acetylene, respectively.

In general, y_1 and y_2 are small compared to 1, and the total molar flowrate, N, can be assumed to be a constant. Equation (1) can be reduced to two equations:

$$r_1\, dx = N d\, y_1 \tag{2}$$

and

$$r_2\, dx = N d\, y_2 \tag{3}$$

but

$$r_1 = \frac{k_1 PC}{R T_G}\left(1 - \frac{y_1}{K_1}\right) \tag{4}$$

and

$$r_2 = \frac{k_2 PC}{R T_G}\left(1 - \frac{y_2}{K_2}\right) \tag{5}$$

where C is the corroding perimeter.

Substituting into (2) and (3), we have

$$\frac{k_1 PC}{R T_G}\left(1 - \frac{y_1}{K_1}\right) dx = N\, d\, y_1 \tag{6}$$

CONFIDENTIAL
RESTRICTED DATA
Atomic Energy Act - 1954

The local rate of surface regression, neglecting erosion effects, can be given by the equation

$$\frac{dr}{dt} = \frac{a P}{R T_G} \left[k_1 \left(1 - \frac{y_1}{K_1} \right) + 2 k_2 \left(1 - \frac{y_2}{K_2} \right) \right] \tag{12}$$

where r is the surface regression in mils, and a is a proportionality constant. At steady-state, the term on the right is a constant if surface regression is small compared to the diameter of the flow channel (this implicitly assumes that the corroding perimeter is a constant). This is true for the case of short reaction times. Thus Equation (12) can be integrated to give the total local wall regression after time Δt

$$\Delta r = \frac{a P}{R T_G} \left[k_1 \left(1 - \frac{y_1}{K_1} \right) + 2 k_2 \left(1 - \frac{y_2}{K_2} \right) \right] \Delta t \tag{13}$$

or

$$\Delta r = \frac{a P}{R T_G} \left(k_1 e^{-\frac{k_1 C P X}{K_1 R T_G N}} + 2 k_2 e^{-\frac{k_2 C P X}{K_2 R T_G N}} \right) \Delta t$$

Finally, to calculate the overall weight loss of graphite, Equation (13) must be integrated along the flow channel

$$\Delta W_T = \beta \int_0^L \Delta r \, d Z = \frac{a' P}{R T_G} \Delta t \int_0^L \left(k_1 e^{-\frac{k_1 C P X}{K_1 R T_G N}} + 2 k_2 e^{-\frac{k_2 C P X}{K_2 R T_G N}} \right) dx$$

which gives

and

$$\frac{k_2 PC}{R T_G}\left(1 - \frac{y_2}{K_2}\right) dx = N\, d y_2 \tag{7}$$

In the case of isothermal reaction, T is a constant along the flow channel; hence, K_2 and K are also constant. In addition, if the pressure does not vary appreciably, Equation (6) can be integrated directly by rewriting them in the form of

$$\frac{k_1 PC}{K_1 N R T_G}\int_0^x dx = \int_0^{y_1} \frac{d y_1}{K_1 - y_1} \tag{8}$$

Similarly,

$$\frac{k_2 PC}{K_2 N R T_G}\int_0^x dx = \int_0^{y_2} \frac{d y_2}{K_2 - y_2} \tag{9}$$

From which one obtains the following for the local concentrations of methane and acetylene:

$$1 - \frac{y_1}{K_1} = e^{-\frac{k_1 C P X}{K_1 R T_G N}} \tag{10}$$

and

$$1 - \frac{y_2}{K_2} = e^{-\frac{k_2 C P X}{K_2 R T_G N}} \tag{11}$$

$$\Delta W_T = a\,N\,\Delta t\left[K_1\left(1 - e^{-\frac{k_1 PCL}{K_1 RT_G N}}\right) + 2K_2\left(1 - e^{-\frac{k_2 PCL}{K_2 RT_G N}}\right)\right] \qquad (14)$$

Using the consistent units indicated in the nomenclature, giving Wt in grams, the constant a should be equal to 3.26×10^5. Equation (14) was used to calculate the weight loss of approximately 12-inches long, unfueled, 19-hole elements. The experimental flowrates and pressures and other conditions are given in Table I. Since the corrosion time was only one minute and the material temperature was constant at 3730°R, the assumptions used in the derivation of Equation (14) are valid in this case. For this particular test, the gas was preheated to 3732°R before entering the test element; hence, the gas and surface temperatures are equal.

CONFIDENTIAL
RESTRICTED DATA
Atomic Energy Act - 1954

APPENDIX III

Non-Isothermal Corrosion With Constant Corroding Perimeters

The flow reaction equations for methane and acetylene are again given here

$$\frac{k_1 P C}{R T_G}\left(1 - \frac{y_1}{K_1}\right) dx = N\, d y_1 \tag{1}$$

and

$$\frac{k_2 P C}{R T_G}\left(1 - \frac{y_2}{K_2}\right) dx = N\, d y_2 \tag{2}$$

In a long flow channel in which the temperature is a function of the axial position x, Equations (1) and (2) cannot be integrated over long distances. However, by taking small finite increments constant temperature and pressure can be assumed for that increment, and a step-wise integration can be carried out to calculate the local methane and acetylene concentrations. This gives the results

$$\left(1 - \frac{y_1}{K_1}\right)_{n+1} = \left(1 - \frac{y_1}{K_1}\right)_n e^{-\frac{k_1 C P \Delta X}{K_1 R T_G N}} \tag{3}$$

and

$$\left(1 - \frac{y_2}{K_2}\right)_{n+1} = \left(1 - \frac{y_2}{K_2}\right)_n e^{-\frac{k_1 C P \Delta X}{K_2 R T_G N}} \tag{4}$$

where n denotes the 7th increment taken with incremental length ΔX. Note that at $n = 0$, y_1 and y_2 are zeros and the methane and acetylene concentrations for subsequent intervals can be readily calculated. The local surface regression rate is than calculated from the equation

$$\frac{dr}{dt} = \frac{aP}{RT_G}\left[k_1\left(1 - \frac{y_1}{K_1}\right) + 2k_2\left(1 - \frac{y_2}{K_2}\right)\right] \tag{5}$$

For the graphite annulus, corrosion occurred on both surfaces of the annulus; consequently, the corroding perimeter remains a constant, and Equation (5) holds for all corrosion times. For the small annular flow passage, the gas temperature was again assumed to be equal to the corroding surface temperature.

CONFIDENTIAL
RESTRICTED DATA
Atomic Energy Act 1954

APPENDIX IV

Non-Isothermal Corrosion and Varying Corroding Perimeter

In the corrosion of uncoated coolant channels, the depth of corrosion relative to the channel diameter is not negligible and the corroding perimeter varies with time. Since the observed local surface regression represents an overall value while the observed rates of corrosion are average values, Equations (4) and (5) in Appendix III must be solved for small time increments. The calculated cumulative regression divided by the total corrosion time is then the average rate of corrosion. Letting the subscript i denote the ith increment in axial length and j the jth time increment, then the solution for the local methane and acetylene concentrations are

$$\left(1-\frac{y_1}{K_1}\right)_{i+1,\,j} = \left(1-\frac{y_1}{K_1}\right)_{i,\,j} e^{-\frac{k_1 C_j P \Delta X}{K_1 R T_G N}} \tag{1}$$

and

$$\left(1-\frac{y_2}{K_2}\right)_{i+1,\,j} = \left(1-\frac{y_2}{K_2}\right)_{i,\,j} e^{-\frac{k_2 C_j P \Delta X}{K_2 R T_G N}} \tag{2}$$

The corresponding rate of surface regression is then

$$\left(\frac{dr}{dt}\right)_{i,\,j} = \frac{\alpha P}{R T_G}\left[k_1\left(1-\frac{y_1}{K_1}\right)_{i,\,j} + 2k_2\left(1-\frac{y_2}{K_2}\right)_{i,\,j}\right] \tag{3}$$

CONFIDENTIAL
RESTRICTED DATA
Atomic Energy Act 1954

where $i = 1, 2, \text{----} L/\Delta X$

$j = 1, 2, \text{----} \tau/\Delta t$

L = total length of the channel

τ = total corrosion time

Equation (3) was used to analyze the corrosion of uncoated coolant channels. Calculated surface (material) and gas temperature distributions and pressure distributions were used.

APPENDIX V

Mechanism of Hydrogenation Reactions

The formation of acetylene by the reaction of hydrogen with graphite can be assumed to follow the following steps:

1) Adsorption of hydrogen on surface active sites:

$$H_2 + -\overset{|}{C}=\overset{|}{C}- \underset{k_o'}{\overset{k_o}{\rightleftharpoons}} -\overset{H}{\overset{|}{C}}=\overset{H}{\overset{|}{C}}- \qquad (1)$$

2) Surface rearrangement (reaction) step:

$$-\overset{H}{\overset{|}{C}}=\overset{H}{\overset{|}{C}}- \underset{k_2'}{\overset{k_2}{\rightleftharpoons}} C_2H_2 \qquad (2)$$

If it is postulated that that surface reaction step is rate-controlling, then the first step is rapid and the surface concentration $-\overset{H}{\overset{|}{C}}=\overset{H}{\overset{|}{C}}-$ is merely the equilibrium concentration:

$$C_{C_2H_2} = K_o (C_v\, p_{H_2})_{eq.} \qquad (3)$$

where K_o is the equilibrium constant for the adsorption step, C_v is the concentration of vacant sites, and p_{H_2} is the partial pressure of hydrogen. The rate of acetylene formation is then

$$\frac{d\, n_{C_2H_2}}{d\, t} = k_2\, C_{C_2H_2} - k_2'\, p_{C_2H_2} \qquad (4)$$

But the equilibrium constant of the second step is given by

$$K_2 = \frac{k_2}{k_2'} = \left(\frac{p_{C_2H_2}}{C_{C_2H_2}}\right)_{eq.} \tag{5}$$

Whence Equation (4) can be written in the form

$$\frac{d\,n_{C_2H_2}}{d\,t} = k_2 K_o C_{v_{eq.}} \left(p_{H_2} - \frac{p_{C_2H_2}}{K_{p_2}}\right) \tag{6}$$

where

$$K_{p_2} = \left(\frac{p_{C_2H_2}}{p_{H_2}}\right)_{eq.} \tag{7}$$

Equation (6) can also be written in terms of concentrations, giving

$$\frac{d\,n_{C_2H_2}}{d\,t} = k_2 K_o C_{v_{eq.}} \left(C_{H_2} - \frac{C_{C_2H_2}}{K_{C_2H_2}}\right) \tag{8}$$

Now if the equilibrium concentration of surface active sites covered is negligible compared to the available active sites, then

$$C_{v_{eq.}} = C_c - C_{C_2H_2} \approx C_o \tag{9}$$

The initial concentration, C_o, is proportional to the gross surface area:

$$C_o = \alpha S \tag{10}$$

Substituting (9) and (10) into Equation (8) yields

$$\frac{d\,n_{C_2H_2}}{d\,t} = \alpha\, k_2\, K_o\, S \left(C_{H_2} - \frac{C_{C_2H_2}}{K_{C_2H_2}} \right) \tag{11}$$

Lumping all the constants into one, k, yields

$$\frac{d\,n_{C_2H_2}}{d\,t} = k\, S \left(C_{H_2} - \frac{C_{C_2H_2}}{H_{C_2H_2}} \right) \tag{12}$$

Following this approach, the rate equation for methane formation can also be derived.

APPENDIX VI

Rates of Diffusion and Corrosion

The mass transfer mechanisms which may conceivably control the rate of corrosion are, 1) diffusion of hydrogen from the bulk stream to the solid–vapor interface, 2) diffusion through the pores, 3) diffusion of reaction products out of the pores, and 4) diffusion of products from the vapor–solid interface to the bulk stream. To compare the rates of diffusion and apparent rates of corrosion, the bulk and pore diffusion of methane shall be calculated and compared with the observed overall rate of methane formation.

The rate of methane formation is given previously by the equation

$$\frac{d\,n_{CH_4}}{d\,t} = \frac{k_1 P}{R T}\left(1 - \frac{y}{K_1}\right) \tag{1}$$

Bulk Diffusion

The rate of bulk methane diffusion can be written in the form

$$\frac{d\,n_{CH_4}}{d\,t} = \frac{D_v P}{\Delta X R T}\,(y^* - y) \tag{2}$$

where D_v is the diffusivity, y^* is the mole fraction methane at the vapor–solid interface, y is the mole fraction methane at a distance ΔX from the vapor–solid interface. Assuming that ΔX is sufficiently great so that $y = 0$, Equation (2) reduces to

$$\frac{d\,n_{CH_4}}{d\,t} = \frac{D_v P}{\Delta X R T}\,y^* \tag{3}$$

Note that if bulk diffusion is assumed rate controlling, then y^* should correspond to the equilibrium mole fraction at the temperature of the vapor-solid interface. This assumption should also give the minimum rate of diffusion. Now the maximum rate of methane formation occurs when y/K_1 is negligible. In this limit, Equation (1) becomes

$$\frac{d\,n_{CH_4}}{dt} = \frac{k_1 P}{RT} \tag{4}$$

From Equations (3) and (4), it becomes evident that it is only necessary to compare k_1 and

$$\frac{D_v y^*}{\Delta X}$$

to determine the relative rates of diffusion and surface reaction.

A typical condition under which methane is the primary reaction product is 2500°R and 600 psia. For these conditions, $k_1 = .0006 \frac{in}{sec}$, $y^* = .19$. Following Bird et. al.,[15] the diffusion coefficient calculated for these conditions in the binary methane-hydrogen is $2.01 \frac{in^2}{sec}$. Comparing bulk diffusion and apparent reaction rates:

Methane Formation: $k_1 = .0006 \frac{in}{sec}$

Diffusion: $\frac{D_v y^*}{\Delta X} = \frac{.382}{\Delta X} \frac{in}{sec}$

It can be readily seen that for any reasonable value of ΔX (given in inches), the rate of diffusion is significantly greater than the rate of surface reaction. Further, it should be recalled that the apparent reaction rate calculated is the maximum value! Since diffusion is more rapid than the apparent rate of reaction, it is obvious that turbulent mass transfer would be even greater!

Pore Diffusion

If the pore diameter is large compared to the mean free path of the diffusing molecules, then the rate of pore diffusion is equal to the rate of bulk diffusion. If the pore diameter is on the order of the mean free path, then Knudsen diffusion occurs. In graphite materials, there exists a wide spectrum of pore diameters, covering a range as wide as 15 to 100,000 angstroms.[16] Nightingale[16] showed that for CSF and AGOT type graphites, the total pore volumes accessible from 15 to 170 A pore diameters is 0.0021 cm^3/g and that which is accessible from 2000 to 100,000 A pore diameters is 0.68 cm^3/g. Since the mean free path of hydrogen is 1600 A and that of methane is on the order of 500 A,[17] it becomes evident that bulk diffusion dominates in the pores. Nevertheless, it would be of interest to compare the rates of bulk diffusion and Knudsen diffusion. The diffusivity for Knudsen diffusion is given by[18]

$$D_k = 9.7 \times 10^3 \, r \sqrt{\frac{T}{M}} \quad \frac{cm^2}{sec} \tag{5}$$

where M is the molecular weight, and r is the pore radius. For the same temperature of 2500°R and using a minimum radius of 7.5 A, the value of Knudsen diffusivity is 0.0638 in^2/sec. Comparing this with the bulk diffusivity shows that the rate of bulk diffusion is at least 32 times greater (if the length of diffusion path, ΔX, is assumed to be equal). However, it is obvious that the rate of Knudsen diffusion is significantly greater than the apparent rate of reaction. It may therefore be concluded that surface reaction is the rate-controlling mechanism.

TABLE I

LASL Corrosion Tests on Unloaded, 19-Hole Hexes

Corrosion Time = 1 min.

Temperature = 1800°C, isothermal tests

Gas preheated to same temperature

Element No.	Wt. Change gm	Mass Flowrate lb/hr	Pressure psig	Length in.
1129A32-97	- 4.4	67	560	12-7/16
1129A13-99	- 9.3	67	1000	12-7/16
1129A40-97	- 7.9	67	1000	12-7/16
1129A2-99	- 6.2	125	550	12-7/16
1129A17-99	- 4.1	67	300	12-7/16
1231AA-4	- 4.5	67	400	12
1231AA-4B	- 5.3	67	650	12-5/8
1231AA-2B	- 6.7	125	550	12-5/8
1231AA-2B	- 6.0	90	550	12-5/8

TABLE II

Corrosion of AUC Annulus
1-1/8 Inch Diameter, .010 Inch Gap

Flowrate	= 1.39×10^{-2} lb/sec
Upstream Pressure	= 550 psig
Pressure Drop	= 420 psi
Total Run Time	= 2 min. 6 sec.

In. From Inlet	T, °R	Corrosion, mils
12		0
15	3912	
18		6
22.5	4632	
24		11
30		26
31	5352	
32.5		50.5
34.5	5892	
35.5		69
37		80
40		85
42.5	> 5892	85.25
45		85
48		83
54		76

TABLE III

Corrosion of Uncoated Coolant Channels

Run 331

Fuel Element AC 89-08390

Run Time = 5 minutes at temperature

Total Weight Loss = 30.7 gm

Total Flowrate = 4.42×10^{-2} lb/sec

Inlet Pressure = 665 psig

Outlet Pressure = 560 psig

X, In. From Cold End	$\bar{T}$, °R	Wall Regression Rate, Mils/Min	
		Channel No. 1	Channel No. 3
10	2600	4.5	3
20	3130	15.5	12.5
30	3650	27.0	38.5
40	4260		44.5
50	4900		
52	4650		

CONFIDENTIAL
RESTRICTED DATA
Atomic Energy Act 1954

TABLE IV

Corrosion of Unlined Support Block* (ATJ Graphite, Sp. Gr. = 1.73)
500 psia

T, °R	Average Corrosion Rate, mg/cm^2-min	Average Wall Regression Rate, mils/min
3732	7	1.59
4103	14	3.18
4272	22	5.0
4452	30	6.82
4642	40	9.10
4952	50	11.37

*Unpublished data from C. A. Landahl, LASL.

SNPO-C
JUL 9 1965
CLASSIFIED

CONFIDENTIAL
RESTRICTED DATA
Atomic Energy Act - 1954